A TECHNIQUE FOR ESTIMATING SYSTEM-WIDE PHASORS IN REAL TIME

Sunil Kabra

Thesis submitted to the Faculty of the
Virginia Polytechnic Institute and State University
in partial fulfillment of the requirements for the degree of

Master of Science
in
Electrical Engineering

APPROVED BY

_____
Dr. Arun G. Phadke, Chairman

_____ _____
Dr. Yilu Liu Dr. Jaime De La Ree

January 1997

Blacksburg, Virginia

A TECHNIQUE FOR ESTIMATING SYSTEM-WIDE PHASORS IN REAL TIME

Sunil Kabra

Committee Chair: Dr. Arun G. Phadke
Department of Electrical Engineering

(ABSTRACT)

The objective of this study is to investigate the application of Synchronized Phasor Measurement techniques in real time estimation of power system phasors. The WSCC System is a very large power system network constituted by a number of electric utilities and power companies. The system was analysed and equivalents developed to suit the purpose of this project. Using these equivalents, the system was simulated for various contingencies to analyze its behaviour. The purpose is to develop a technique for estimating the voltage phasors at all major substation buses of the system from a limited number of available real time phasors at a fixed set of substations. The system load flow was computed for various possible loading situations. Various loading patterns were created around a base summer time load flow case. Using the results from these computations, an empirical relationship was developed between phasors from a fixed set of locations and the unknown phasors at the rest of the system buses.

ACKNOWLEDGEMENTS

I am very grateful to my research advisor Dr. Arun Phadke for his guidance, support and help without which it would not have been possible for me to complete ths research. I am also grateful to my comittee members Dr. Jaime De La Ree and Dr. Yilu Liu for helping me out on various occasions with their esteemed knowledge and valuable guidance. Lastly, I am thankful to all my lab partners and fellow students who have helped me with their valuable company and moral support.

TABLE OF CONTENTS

1. INTRODUCTION 1-1

1.1 INTRODUCTION 1-1
1.2 PHASOR MEASUREMENT PRINCIPLES 1-1
1.3 WSCC POWER SYSTEM 1-4

2. PMU PLACEMENT ON WSCC SYSTEM 2-1

2.1 INTRODUCTION 2-1
2.2 DUAL SEARCH METHOD FOR PMU PLACEMENT 2-2
2.3 RESULTS OF THE DUAL SEARCH STUDIES 2-4
2.3.1 APS and SRP SYSTEM 2-4
2.3.2 LOS ANGELES DEPARTMENT OF WATER AND POWER 2-7
2.3.3 PACIFIC GAS AND ELECTRIC (WITH SMUD) 2-9
2.4 COHERENCY BASED CLUSTERING 2-13
2.4.1 Coherency Based Algorithm: 2-13
2.5 FINAL PLACEMENT PLAN 2-17

3. ESTIMATION OF SYSTEM PHASORS 3-1

3.1 INTRODUCTION 3-1
3.2 THE AVAILABLE PHASORS 3-2
3.3 MATHEMATICAL FORMULATION 3-9
3.4 ESTIMATION RESULTS ON SAMPLE CASES 3-11
3.5 LINE OUTAGE STUDIES 3-28
3.6 RESULTS OF LINE OUTAGE STUDIES 3-29
3.7 SERIES COMPENSATOR BUSES: 3-41
3.8 WINTER TIME LOAD FLOW CASE 3-42

4. CONCLUSION AND FUTURE WORK 4-1

4.1 CONCLUSION 4-1
4.2 FUTURE WORK 4-1

5. REFERENCES 5-1

LIST OF FIGURES

FIGURE 1.1 BLOCK DIAGRAM OF A SYNCHRONIZED PHASOR MEASUREMENT UNIT 1-3
FIGURE 1.2 WSCC AREA MAP AND PMU LOCATIONS 1-4
FIGURE 3.1 WSCC SYSTEM DIVIDED INTO FIVE AREAS TO GENERATE VARIOUS LOAD FLOW CASES 3-5
FIGURE 3.2 TEST CASE 1 - ANGLES 3-11
FIGURE 3.3 TEST CASE 2 - ANGLES 3-12
FIGURE 3.4 TEST CASE 3 - ANGLES 3-13
FIGURE 3.5 TEST CASE 4 - ANGLES 3-14
FIGURE 3.6 TEST CASE 5 - ANGLES 3-15
FIGURE 3.7 TEST CASE 6 - ANGLES 3-16
FIGURE 3.8 TEST CASE 7 - ANGLES 3-17
FIGURE 3.9 TEST CASE 8 - ANGLES 3-18
FIGURE 3.10 TEST CASE 1 - VOLTAGES 3-19
FIGURE 3.11 TEST CASE 2 - VOLTAGES 3-20
FIGURE 3.12 TEST CASE 3 - VOLTAGES 3-21
FIGURE 3.13 TEST CASE 4 - VOLTAGES 3-22
FIGURE 3.14 TEST CASE 5 - VOLTAGES 3-23
FIGURE 3.15 TEST CASE 6 - VOLTAGES 3-24
FIGURE 3.16 TEST CASE 7 - VOLTAGES 3-25
FIGURE 3.17 TEST CASE 8 - VOLTAGES 3-26
FIGURE 3.18 LINE OUTAGE CASE 1 - ANGLES 3-29
FIGURE 3.19 LINE OUTAGE CASE 2 - ANGLES 3-30
FIGURE 3.20 LINE OUTAGE CASE 3 - ANGLES 3-31
FIGURE 3.21 LINE OUTAGE CASE 4 - ANGLES 3-32
FIGURE 3.22 LINE OUTAGE CASE 5 - ANGLES 3-33
FIGURE 3.23 LINE OUTAGE CASE 6 - ANGLES 3-34
FIGURE 3.24 LINE OUTAGE CASE 1 - VOLTAGES 3-35
FIGURE 3.25 LINE OUTAGE CASE 2 - VOLTAGES 3-36
FIGURE 3.26 LINE OUTAGE CASE 3 - VOLTAGES 3-37
FIGURE 3.27 LINE OUTAGE CASE 4 - VOLTAGES 3-38
FIGURE 3.28 LINE OUTAGE CASE 5 - VOLTAGES 3-39
FIGURE 3.29 LINE OUTAGE CASE 6 - VOLTAGES 3-40
FIGURE 3.30 SERIES CAPACITOR BUSES 3-41
FIGURE 3.31 WINTER CASE ESTIMATED AND ACTUAL VOLTAGES 3-43
FIGURE 3.32 ERROR IN ESTIMATION OF WINTER CASE VOLTAGES 3-44
FIGURE 3.33 WINTER CASE ESTIMATED AND ACTUAL ANGLES 3-44
FIGURE 3.34 ERROR IN ESTIMATION OF WINTER CASE ANGLES 3-45
FIGURE 3.35 WINTER CASE ANGLES ESTIMATED USING NEW A-MATRIX 3-46
FIGURE 3.36 ERROR IN ESTIMATION OF ANGLES WITH THE NEW A-MATRIX 3-46
FIGURE 3.37 TEST CASE 1 ANGLES ESTIMATED USING THE NEW A-MATRIX 3-47
FIGURE 3.38 ERROR IN ESTIMATION OF TEST CASE 1 ANGLES WITH THE NEW A-MATRIX 3-48
FIGURE 3.39 ERROR IN ESTIMATION OF TEST CASE 1 ANGLES WITH THE OLD A-MATRIX 3-49

LIST OF TABLES

TABLE 2.1 APS & SRP - OPTIMAL PMU LOCATION FOR COMPLETE OBSERVABILITY 2-5
TABLE 2.2 APS & SRP - OPTIMAL PMU LOCATION WITH FORCED PLACEMENT 2-6
TABLE 2.3 LADWP - OPTIMAL PMU LOCATION FOR COMPLETE OBSERVABILITY 2-7
TABLE 2.4 LADWP - OPTIMAL PMU LOCATION WITH FORCED PLACEMENT 2-8
TABLE 2.5 PG&E - OPTIMAL PMU LOCATION FOR COMPLETE OBSERVABILITY 2-9
TABLE 2.6 PG&E - OPTIMAL PMU LOCATION WITH FORCED PLACEMENT 2-11
TABLE 2.7 FINAL PLACEMENT OF PMUS ON THE REDUCED BUS SET OF WSCC 2-17
TABLE 3.1 THE AVAILABLE PHASORS 3-3
TABLE 3.2 AREAWISE LOAD AND GENERATION 3-6
TABLE 3.3 CASES USED TO GENERATE THE A-MATRIX 3-7
TABLE 3.4 DESCRIPTION OF TEST CASES USED AS EXAMPLES 3-8

1.

INTRODUCTION

1.1 Introduction

The purpose of this study is to show that under normal operating conditions the voltage phasors across a power system network move in definitive patterns relative to each other. Given a set of all possible loading situations, this relationship between the phasors of a system can be studied and expessed as an equation of an appropriate order. This study attempts to show that as simple as a linear expression can be sufficient to define the relationship among the phasors of a system. However, the expression and its order are characteristic of a system and individual studies have to be carried out for each system to develop the appropriate relationship among phasors.

The concept of phasors is very useful in describing the behavior of a power system in its steady state as well as in transient state. Although phasors are better understood as representing a steady state sinusoidal waveform, phasor movements can be used to derive a variety of information about the transient state of a power system [1]. Phasor measurement technologies have undergone many changes, first with the advent of digital electronic systems and then with the increasing need for synchronized phasor measurements at different points of large power systems. The principles of phasor measurement are described in the following section.

1.2 Phasor Measurement Principles

In digital systems, phasors are computed by taking discrete samples of a waveform at fixed intervals. If the number of intervals in one time period are N, then the fundamental

frequency component of the Discrete Fourier Transform (DFT) is calculated according to the relation

$$X = \frac{\sqrt{2}}{N}\sum_{k=1}^{N} x_k e^{-j2\Pi k/N} \tag{1.1}$$

where X is the phasor, and x_k are the samples of the waveform. Phasors can be measured for each of the three phases, and the positive sequence phasor X_1 computed as follows:

$$X_1 = \frac{1}{3}\left(x_a + a x_b + a^2 x_c\right), \quad a = e^{j2\Pi/3} \tag{1.2}$$

A Phasor Measurement Unit derives its inputs from the secondary sides of the three phases of a potential or current transformer and outputs the corresponding positive sequence voltage or current phasor. In the context of power system monitoring and control, positive sequence measurements are used more often than the three phase quantities. In a large system, control decisions have to be based upon a number of phasors from different points systemwide. Hence the need for synchronized phasor measurements. The phasors are time stamped using a Global Positioning System (GPS) satellite transmissions. Figure 1.1 shows a functional diagram of a phasor measurement unit. The PMUs are equipped with GPS receivers to obtain the zonal timing signals. The PMUs can be adjusted for different time zones to yield conformity in time stamping at different places.

Synchronized phasor measurements have a huge potential of application in power systems. To name, a few applications are:

- Accurate Measurement of Frequency and Magnitude of Voltages and Currents.
- State Estimation
- Prediction of Instability
- Adaptive Relaying

- Centralized Control and Monitoring

These applications require the PMUs to communicate with a host computer and thus the communication links become an important concern. Most applications in power systems involve modes of oscillations which range from 0 to 5 Hz in frequency and thus time delays of more than 30 ms are not acceptable for control purposes. With the advent of advanced modems and communication links, it is possible to keep communication and processing delays under the required limit.

To summarize our discussion on the Phasor Measurement Units, it is reasonable to assume that synchronized phasor measurements will serve the needs of all monitoring and control functions in power system control centers in future. This technology has the potential of becoming a standard form of all power systems measurements.

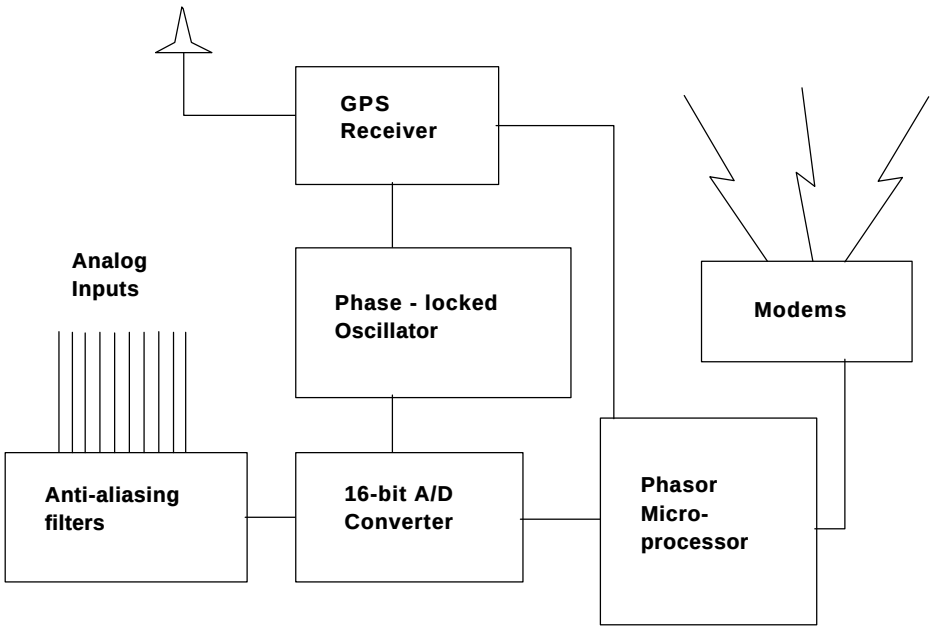

Figure 1.1 Block Diagram of a Synchronized Phasor Measurement Unit

1.3 WSCC Power System

The system on which these studies were done is a network of small power systems sharing power through various inter-ties. The system stretches across the western United States from the coast to the midwestern states. The system area map is shown in Figure 1.2 and the locations of PMU sites are also shown.

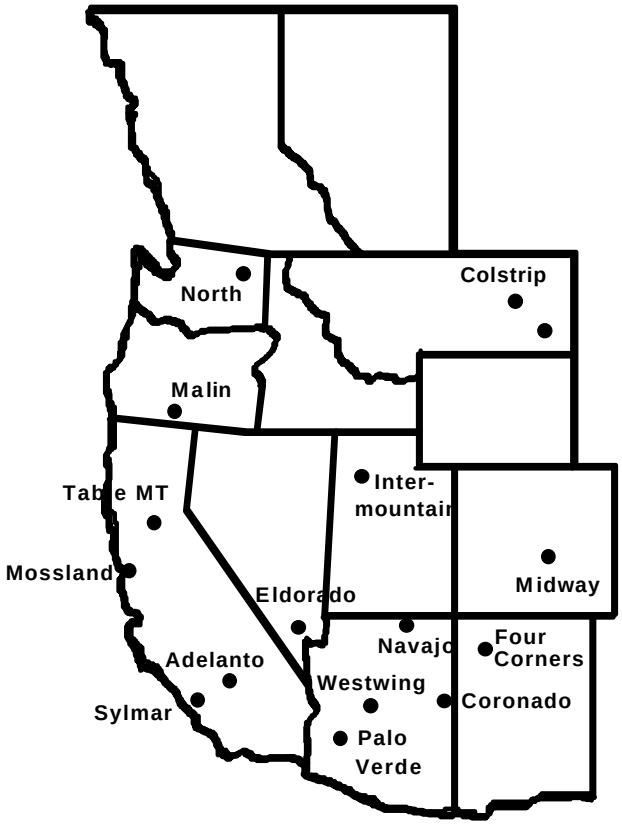

Figure 1.2 WSCC Area Map and PMU Locations

2.

PMU PLACEMENT ON WSCC SYSTEM

2.1 Introduction

The system was first analysed for a PMU placement plan to best utilize the limited resources available while trying to get a good overall picture of the system state at the same time. This chapter concentrates on the PMU placement and system clustering algorithms used on each of the collaborating companies of the WSCC system. The algorithms shall first be discussed in detail followed by the implementation and results of studies on individual system components. However, the feasibility of implementation of a complete placement plan in its entirety was low considering the cost of equipment and other requirements. It is practical to assume that in a network, PMU placement will evolve in time. All the buses cannot be equipped with PMUs in the early stages. The objective of this study is to investigate a useful and convenient placement with a limited number of PMUs available at hand. One consideration is to plan a strategy for evolution which would lead to complete observability of the positive sequence voltages at all network buses. Another consideration is to place the PMUs so that significant dynamic phenomena can be observed. Both of these approaches are discussed next.

In the first approach to the site selection problem, a placement plan was developed on the basis of complete system observability. A Dual Search method [3] was used to find a minimal placement plan with complete observability across the system. The availability of communication links was then investigated and the observability studies were repeated with forced PMU placement on the sites with available communication links. In the second approach, the system was subjected to a coherency based clustering algorithm to identify significant generation sites and examine the possibility of reducing the system network by clustering generations and deducing equivalents. Three networks, namely PG&E, APS-

SRP and LADWP had supplied the system data for observability studies. The Zaborsky algorithm was used to cluster the same three networks on the basis of slow coherency. Towards the end of this chapter, the final PMU sites, after taking into consideration all the factors mentioned above have been listed.

2.2 Dual Search Method for PMU Placement

This method aims at finding the minimal set of PMUs which ensures complete observability of the system network. The algorithm proceeds in three stages.

- An initial set of placements is first developed by a graph theoratic procedure. The principle behind the graph theory-based method is to place a PMU at a starting bus and perform an exhaustive search of all adjacent buses and lines which can be observed by this PMU. Once the boundary limits for one PMU are found, a second PMU is placed into the network and a second exhaustive search for the buses and lines which can be observed is made. The graph theoratic solution marks the upper bound on the number of PMUs. Then a modified bisecting search finds a reduced number of PMUs which is then passed to the simulated annealing method for observability test.
- The simulated annealing method attempts to identify the placement set which minimizes the unobserved region of the system. It returns the optimal placement set for the number of PMUs decided by the bisecting search and also the number of unobserved buses. After a number of such trials the bisecting search has a whole set of number of PMUs. For some of these, the system is observable and for the rest it is not. Accordingly the bisecting search arrives at a number for which the system is observable, but for a number less by one the system is not observable. The philosophy of the modified bisecting search is to minimize the number of trials required to obtain this number.
- Finally for this number of PMUs the simulated annealing method comes up with the best placement for complete observability. The simulated annealing

proceeds in this way. For the number of PMUs provided by the bisecting search, first a random placement set is selected which is sequentially modified by reallocating one PMU at a time. Each new placement set is formed by randomly chosing a PMU in the present placement set and moving it to a randomly chosen new bus. At each stage, the no of unobserved buses is evaluated and compared with the previous set to determine if there is a decrease in the number of unobserved buses. If so, the new placement set replaces the old. Otherwise, the last selected PMU is returned to the previous bus.

A FORTRAN program was developed at Virginia Tech. by T. Baldwin and L. Milli and M. Boisen using this algorithm. This program requires the system topological data including the load, injection and generation at each bus and the type of that bus. The program accepts data in the IEEE format. the program carries a provision of forcing placement of PMUs at selected buses initially. This feature is helpful in dealing with already available communication links at some substations. The available communication links data was made available by the participating utility companies.

These data initially in the WSCC format have been converted into the IEEE format using the EPRI Powerflow and DTAC set of programs. The power flow program does not solve the DC network of any system. Hence, the DC part had to be deleted from each system and their line flows were appropiately incorporated in the data of the AC buses connected to the DC network.

The PGE and SMUD combined system has 845 buses. Placing PMUs for observability of all these buses is impractical from the point of view of cost involved. Hence the system was reduced by eliminating all buses under 115 kV and modelling their contribution to generation and load as injections to the 115 kV and higher buses which are connected to these buses.

The dual search method may not yield a minimum number of PMUs required for observability, but it reduces the simulation time and effort significantly. The task of finding a minimal set of PMUs for complete observability for a big system can otherwise be gigantic. Moreover, the results of dual-search algorithm are satisfactorily close to the minimum set. Typically, the ratio of number of PMUs to the total number of buses is about 20%.

2.3 Results of the Dual Search Studies

The results of the dual search method applied on the three systems of Pacific Gas & Electric (PG&E), Arizona Public Service Company (APS) & Salt River project (SRP) and Los Angeles Department of Water and Power (LADWP) are as follows. No studies were performed on the Bonneville Power Administration (BPA) system as per their request. Southern California Edison (SCE) joined this project at a later date, so the PMU placement data for their system could not be included in this report. In each case, first the optimal PMU placement was found for the system with no forced placement of PMUs at any bus and then forced placements were used at buses which were indicated as being equipped with communication links.

2.3.1 APS and SRP SYSTEM

The system AC buses are not all in one network. Two AC buses CELILO 230 and CELILO 500 are connected to the system through a DC network. The above study was carried out by eliminating these buses and hence one additional PMU has to be placed at either of the two buses mentioned above.

No Forced Placement used in this Case

NO. OF BUSES = 193

NO. OF LINES = 317

Table 2.1 APS & SRP - Optimal PMU Location for Complete Observability

Bus No.	Bus Name	Bus No.	Bus name
2	AGUAFRIA230.	103	MEAD 230.
11	AMRAD 345.	108	MIGUEL 500
15	AULT EQ345.	112	MOHAVE 500.
16	B-A 345.	118	NAVAJO 500.
18	BENLOMND 345	128	PALOVRDE500.
26	CAMP WIL 345	139	PNPKAPS 230.
29	CHOLLA 500.	144	PRECHCYN345.
36	CORONADO500.	145	REDBUTTE 345
39	CRAIG 230.	147	RINALDI 230.
44	CTRYCLUB230.	151	SAN JUAN345.
62	FLAGSTAF345.	155	SERRANO 500.
66	FOURCORN230.	168	SPRINGR 345.
67	FOURCORN345	169	STA E 500.
72	GOLDFELD230.	174	THUNDRST230.
73	GRANDJCT345.	175	TORTOLIT500.
87	INTERMT 345.	177	VAIL 345.
93	KYRENE 230.	182	VINCENT 500.
95	LIBERTY 230.	187	WESTMESA345.
100	LUNA 345.		

STATISTICS

NUMBER OF PMUs - 38

PMU TO TOTAL BUS RATIO - 0.194

Forced placement of PMUs used in this case at the following five buses:

1. FOURCORN345.
2. CORONADO500.
3. NAVAJO 500.
4. PALOVRDE500.
5. PNPKAPS 230.

Table 2.2 APS & SRP - Optimal PMU Location with Forced Placement

Bus No.	Bus Name	Bus No.	Bus Name
36	CORONADO500.	67	FOURCORN345.
118	NAVAJO 500.	128	PALOVRDE500.
139	PNPKAPS 230.	16	B-A 345.
62	FLAGSTAF345.	174	THUNDRST230.
87	INTERMT 345.	29	CHOLLA 500.
93	KYRENE 230.	15	AULT EQ345.
39	CRAIG 230.	187	WESTMESA345.
100	LUNA 345.	26	CAMP WIL 345
66	FOURCORN230.	44	CTRYCLUB230.
103	MEAD 230.	2	AGUAF RIA230.
177	VAIL 345.	11	AMRAD 345.
112	MOHAVE 500.	150	SAGUARO 500.
95	LIBERTY 230.	108	MIGUEL 500
182	VINCENT 500.	168	SPRINGR 345.

Continued... (APS & SRP - Optimal PMU Location with Forced Placement)			
22	BORAH EQ 345	144	PRECHCYN345.
73	GRANDJCT345.	169	STA E 500.
155	SERRANO 500.	160	SILVERKG34.5
147	RINALDI 230.	145	REDBUTTE 345
151	SAN JUAN345.		

STATISTICS

NUMBER OF PMUs - 38

PMU TO TOTAL BUS RATIO - 0.197

2.3.2 LOS ANGELES DEPARTMENT OF WATER AND POWER

No forced placement has been used in this case.

NO. OF BUSES = 97

NO. OF LINES = 170

Table 2.3 LADWP - Optimal PMU Location for Complete Observability

Bus No.	Bus Name	Bus No.	Bus Name
7077	STA KLD 138	7058	STA B 138
7054	SCATERGD 138	7023	HARB4G 13.8
7049	PP 2 G 7.50	7067	STA E 230
7035	INTMT345 345	7015	HAYNES 230
7106	TAPDWP 287	7083	SYLMARLA 230
7022	HARB3G 13.8	7064	STA CLD 138
7088	VALLEY 138	7006	CASTAIC 230
9213	ARDEN 230	7050	RINALDI 230

STATISTICS

NUMBER OF PMUs - 16

PMU TO TOTAL BUS RATIO - 0.164

Forced Placement used in this case at the following buses:

1. Adelanto 500 kV
2. Intermt 345 kV
3. McCullgh 500 kV

Table 2.4 LADWP - Optimal PMU Location with Forced Placement

Bus No.	Bus Name	Bus No.	Bus Name
7000	ADELANTO 500	7035	INTMT345 345
7038	MCCULLGH 500	7015	HAYNES 230
7050	RINALDI 230	7011	HARB 138
7070	STA G 230	9026	DRY LAKE 230
7024	HARB5G 13.8	7058	STA B 138
7006	CASTAIC 230	7054	SCATERGD 138
7042	OLIVE 1 115	7088	VALLEY 138
7027	STA Q 34.5	7077	STA KLD 138
7161	CELILO 230		

STATISTICS

NUMBER OF PMUs - 17

PMU TO TOTAL BUS RATIO - 0.175

2.3.3 PACIFIC GAS AND ELECTRIC (WITH SMUD)

No forced placement has been used in this case.

NO. OF BUSES = 377
NO. OF LINES = 592

Table 2.5 PG&E - Optimal PMU Location for Complete Observability

Bus No.	Bus Name	Bus No.	Bus Name
570	PITSBURG230.	240	FRBSTNTP115
678	TABLE MT230.	753	WILSON 230.
654	SOLEDAD 115.	24	SHASTA 230.
647	SN LS OB115.	81	BELLOTA 230.
422	MC CALL 230.	540	PANOCHE 230.
245	FULTON 115.	351	HUMBOLDT115.
228	FGRDN T1230.	43	PINE FLT230.
474	MORROBAY230.	791	UNIONVLY230.
806	ORANGEVL230.	486	MPE TAP 115.
808	EAST CTY115.	511	NEWARK 115.
459	MIDWAY 500.	249	G13TT1_8230.
480	MOSSLND2115.	31	TRACY 230.
1	MAXWELL 500.	383	KERN OIL115.
468	MORAGA 115.	815	STA. A 115.
263	GATES 1M230.	601	RIO OSO 115.
697	TESLA E 230.	165	COTWDPGE115.
594	RALSTON 230.	610	ROSSMOOR230.

Continued... (PG&E - Optimal PMU Location for Complete Observability)			
251	G16T0_2 230.	111	C.COSTA 230.
578	POE 230.	19	KWICK MP115.
354	IGNACIO 230.	803	HEDGE 230.
752	WHLR R 1230.	499	MTCALF 2115.
801	EL	384	KERN PP 230.
622	SANMATEO115.	606	ROCK CRK230.
44	SN LS PP230.	309	GYF1T1_7230.
580	PO	661	SPRNG GJ115.
336	HIGHLNDS115.	118	CARIBOU 115.
560	PIT	725	USWP-RLF230.
418	MANTECA 115.	679	TABLE MT500.
571	PLACER 115.	466	MONTAVIS230.
743	WARNERVL230.	12	FOLSOM 230.
814	SOUTHCTY115.	284	GEYSR14 230.
549	PEABDY B230.	220	EMBRCDRE230.
252	G9CRT0_4230.	699	TIGR CKM230.
35	BUENAVTP230.	568	PIT 7 230.
457	MIDWAY 115.	287	GEYSR18 230.
553	PIT 1 230.	8	J.F.CARR230.
729	VACA-DIX230.	544	PARKR 230.
400	LE GRAND115.	300	GREGG 230.
761	WND MSTR230.	332	HERNDON 115.
286	GEYSR17 230.	562	PIT 5 JT230.

STATISTICS

NUMBER OF PMUs - 80

PMU TO TOTAL BUS RATIO - 0.212

Forced Placement used in this case at the following buses:

1. Midway 500.
2. Mossland500.
3. Table MT500.

Table 2.6 PG&E - Optimal PMU Location with Forced Placement

Bus No.	Bus Name	Bus No.	Bus Name
459	MIDWAY 500.	475	MOSSLAND500.
679	TABLE MT500.	126	CC SUB 230.
654	SOLEDAD 115.	62	ASHLAN 230.
170	CR1T3_18230.	571	PLACER 115.
729	VACA-DIX230.	553	PIT 1 230.
252	G9CRT0_4230.	300	GREGG 230.
661	SPRNG GJ115.	566	PIT 6 JT230.
17	KESWICK 230.	466	MONTAVIS230.
596	RAVENSWD230.	245	FULTON 115.
457	MIDWAY 115.	814	SOUTHCTY115.
478	MOSSLND1115.	699	TIGR CKM230.
602	RIO OSO 230.	240	FRBSTNTP115.
356	IGNCIO M230.	220	EMBRCDRE230.

Continued... (PG&E - Optimal PMU Location with Forced Placement)			
400	LE GRAND115.	19	KWICK MP115.
456	MIDLFORK230.	284	GEYSR14 230.
80	BELLOTA 115.	697	TESLA E 230.
544	PARKR 230.	127	CCPA1 230.
33	TRINITY 230.	251	G16T0_2 230.
24	SHASTA 230.	11	FOLSM PH115.
8	J.F.CARR230.	122	CASCADE 115.
351	HUMBOLDT115.	336	HIGHLNDS115.
562	PIT 5 JT230.	410	LOSBANOS230.
118	CARIBOU 115.	580	POTRERO 115.
450	MESA_PGE115.	755	WILSON B115.
817	STA. D 115.	743	WARNERVL230.
570	PITSBURG230.	606	ROCK CRK230.
560	PIT 4 JT230.	49	WHLR R2J230.
249	G13TT1_8230.	71	BALCH 230.
81	BELLOTA 230.	791	UNIONVLY230.
1	MAXWELL 500.	111	C.COSTA 230.
511	NEWARK 115.	622	SANMATEO115.
384	KERN PP 230.	601	RIO OSO 115.
498	MTCALF 1115.	725	USWP-RLF230.
422	MC CALL 230.	761	WND MSTR230.
385	KERN PWR115.	332	HERNDON 115.

Continued... (PG&E - Optimal PMU Location with Forced Placement)			
474	MORROBAY230.	752	WHLR R 1230.
803	HEDGE 230.	540	PANOCHE 230.
212	EGLE RCK115.	79	BELDEN 230.
678	TABLE MT230.	205	DUMBARTN115.
31	TRACY 230.	806	ORANGEVL230.
808	EAST CTY115.	128	CCPA2 230.
468	MORAGA 115.	809	ELVERTAS115.
263	GATES 1M230.		

STATISTICS

NUMBER OF PMUs - 85

PMU TO TOTAL BUS RATIO - 0.225

2.4 Coherency Based Clustering

It has been observed that in large power systems, groups of stiffly interconnected machines show coherent motion in the event of a disturbance. Broadly speaking, the system dynamics can be seperated into fast and slow dynamics. The slow dynamics consist of inter-group oscillations whereas the the machine oscillations within a group constitute fast dynamics. The fast and the slow dynamics have a moderate amount of influence on each other. This phenomenon has been given the name of ‘slow coherency’. Coherency based clustering is the technique of identifying the clusters of machines which exhibit slow coherency.

2.4.1 Coherency Based Algorithm:

This algorithm proceeds as follows:

1. Solve the load flow of the system.
2. Model the load flows as constant impedances and update [Ybus] by including these impedances in its diagonal terms.
3. Update [Ybus] to include transient reactances and create an extended matrix,

$$\begin{matrix} & \text{NBUS} & \text{NGEN} \\ [Y_{ext}] = & \begin{bmatrix} [Y_{bus}] & [Y_{12}] \\ [Y_{21}] & [Y_{22}] \end{bmatrix} & \begin{matrix} \\ \text{NBUS} \\ \text{NGEN} \end{matrix} \end{matrix} \tag{2.1}$$

4. Obtain a reduced Y matrix (reduced to the internal nodes) by Kron reduction.

$$[Y_{red}] = [Y_{22}] - [Y_{21}][Y_{bus}]^{-1}[Y_{12}] \tag{2.2}$$

5. Calculate the vector of internal voltages $\vec{\mathbf{E}} = \vec{E} \angle \vec{\delta}$
6. Calculate the Jacobian for the reduced system:

$$[K] = \begin{bmatrix} \frac{\partial \vec{P}}{\partial \vec{\delta}} \end{bmatrix} \tag{2.3}$$

$$\text{where } \vec{P} = \begin{bmatrix} P_{g_1} \\ M \\ M \\ P_{g_{ngen}} \end{bmatrix} \text{ and } \vec{\delta} = \begin{bmatrix} \delta_1 \\ M \\ M \\ \delta_{ngen} \end{bmatrix} \tag{2.4}$$

where P's are the electric power output at each generation bus and δ's are the generator rotor angles .

$$\frac{\partial P_k}{\partial \delta_n} = -E_k E_n Y_{kn} \sin(\theta_{kn} + \delta_n - \delta_k), \quad n \neq k \tag{2.5}$$

where θ_{kn} is the angle of the element (k,n) in $[Y_{red}]$.

$$\frac{\partial P_k}{\partial \delta_k} = \sum_{\substack{n=1, \\ n \neq k}}^{ngen} - \frac{\partial P_k}{\partial \delta_n} \tag{2.6}$$

This Jacobian is singular because all the rotor angles are arbitrary upto an additive constant (the reference angle).

7. The linear dynamic model is $\frac{\partial \vec{\Delta d}}{\partial t} = [A].\vec{\Delta d}$, (2.7)

where $[A] = -[M]^{-1}.[K]$,

$[M] = \text{diag}\left(M_1 K \; K \; K \; M_{ngen}\right)$,

and $M_i = 2 H_i / w_s$, H_i is the inertia constant of machine i.

[A] is diagonally dominant since, $\left|a_{ii}\right| = \sum_{\substack{j=1, \\ j \neq i}}^{ngen} \left|a_{ij}\right|$

8. Scale [A] by dividing every element by the largest element in the diagonal of [A].
9. Calculate the matrix [B_i], which is of the same order as [A], i.e., (NGEN x NGEN). The row-i in [B_i] is the sorted index of row i of A from smallest to largest absolute value, i.e., the element bi(i,1) is the column of the element with the smallest absolute value in row i of [A], b_i(i,2) is the column of the element in row-i whose absolute value is the second in ascending order, etc.
10. Calculate the reduced incidence matrix, [C] as follows:

i) $c(i,j) = \begin{cases} 0, \text{if } a(i,j) = 0 \\ \\ 1, \text{otherwise.} \end{cases}$

ii) Weak connections in [A] are cut in [C] as follows: define the element with the smallest absolute value in row i of [A] as a(i,j1), where j1 = b_i(i,1). If |a(i,j1)| $\leq a$, set c(i,j1) = 0. Now, get the next element of [B_i] in row i, name it j2 and if the sum |a(i,j1)| + |a(i,j2)| $\leq a$, set c(i,j2) = 0. Repeat this while sum

$|a(i,j_1)|$ + ... + $|a(i,j_m)|$ is $\leq \alpha$

iii) Symmetrize [C], i.e., if c(i,j) $\neq$ c(j,i) then set c(i,j) = c(j,i) = 1.

iv) Cluster the reduced, symmetrized incidence matrix [C] into a block diagonal form of disjoint subsystems:

$[C] = \text{diag}\ ([C^{kk}])$

At this stage, for a range of α, such that $\alpha_m \le \alpha \le \alpha_M$, the [C] matrix would look like,

$$[C] = \begin{bmatrix} 1 & 1 & 0 & 0 & 0 & 0 & 0 \\ 1 & 1 & 0 & 0 & 0 & 0 & 0 \\ 0 & 0 & 1 & 1 & 1 & 0 & 0 \\ 0 & 0 & 1 & 1 & 1 & 0 & 0 \\ 0 & 0 & 1 & 1 & 1 & 0 & 0 \\ 0 & 0 & 0 & 0 & 0 & 1 & 1 \\ 0 & 0 & 0 & 0 & 0 & 1 & 1 \end{bmatrix}$$

The quantity α is arbitrarily selected. The number of clusters will depend on the value of α and the characteristics of the network. If α is smaller than the smallest term $|a_{ij}|$ in A, then A is not α-decomposable for this α and the result is one cluster, the entire network. If α=1 each cluster will have a single machine. Hence, α has to be selected between the smallest term in A and 1. In this seven machine example (the [C] matrix shown above), there are three distinct clusters of machines which form three areas of coherency.

A solution of the clustering algorithm is defined as being meaningful if

$$2\{\alpha_m/\alpha_M\} << 1 \quad \text{and} \quad N\{\alpha_m/\alpha_M\} << 1 \tag{2.8}$$

where N is the number of clusters given by the algorithm for $\alpha_m < \alpha < \alpha_M$.

Hence, for a good clustering solution, α should be small and the range of α which gives a constant number of clusters should be large. Also, a small value of N compared to the number of generation buses in the system indicates effective clustering. However, in both the PG&E and APS (including SRP) systems, the algorithm gives a constant number of clusters for very small ranges of α and by the time a constant value of N is reached, N is almost equal to the number of generation buses. This is to be expected since the system used has already been equivalized.

The PG&E and the APS (and SRP) systems were examined for clustering on the basis of coherency. The algorithm described was used for clustering. However, in the terminology of this algorithm a meaningful clustering solution does not exist in either of the two cases. This means that for dynamic studies the complete system must be retained.

Since no dynamic model data was available for the Los Angeles Department of Water and Power (LADWP), no coherency analysis was performed on that system.
In conclusion, it is clear that the reduced models provided for these studies are already well-clustered from the point of view of dynamics, and no further dynamic reduction is advisable. This being the case, the site placement is solely controlled by the availability of communication facilities and observability for state estimation.

2.5 Final Placement Plan

The final placement of PMUs selected at the initial stage is shown below.

Table 2.7 Final Placement of PMUs on the Reduced Bus Set of WSCC

BPA	1.	Malin 500-kV
	2.	North 500-kV (Grand Coulee)
	3.	Montana 500-kV (Colstrip)
	4.	Big Eddy 500-kV
PG&E	5.	Midway 500-kV
	6.	Table MT 500-kV
	7.	Mossland 500-kV
	8.	Tevatr 500-kV
APS	9.	Fourcorn 345-kV
	10.	Navajo 500-kV
	11.	Paloverde 500-kV
	12.	Coronado 500-kV
	13.	Westwing 500-kV (for Pinnacle Peak 345-kV)
LADWP	14.	Adelanto 500-kV
	15.	Intermt 345-kV
	16.	Sylmarla 230-kV
	17.	Eldorado 500-kV (for McCullugh 500-kV)

3.

ESTIMATION OF SYSTEM PHASORS

3.1 Introduction

As evident from the placement studies, the determining factor in PMU placement on the WSCC system has been the availability of communication links thereby making the nature of placement evolutionary in concept. Due to the evolutionary nature of PMU installation, not enough bus voltages can be directly measured. However, several applications require the voltage phasors at all system buses. Hence, a technique is needed to produce a complete system state vector from a few real measurements. This chapter provides a technique for acheiving this.

The angles of bus voltage phasors in a system are governed by the load pattern and the angles of closely placed buses tend to be coherent. Hence, by taking into account a number of possible load scenarios, an empirical relationship between the phasors of a central bus in a neighborhood, and the neighboring buses can be derived for each cluster of closely placed or tightly connected buses. The same reasoning has been applied here to estimate phasors at all unobserved buses of the system. The voltage magnitude of each unknown phasor in the system is assumed to be a linear combination of magnitudes of PMU bus voltages and the voltage angle of each unknown phasor in the system is assumed to be a linear combination of voltage angles at PMU buses. The coefficients of the linear relationship are determined by simulating a number of different load patterns on the network, and doing a least squares fit to obtain the coefficients of the connection matrix. This method was first applied to the IEEE 39 bus system. After getting encouraging results, the same technique was used for estimation in the WSCC system. Having obtained satisfactory results with linear correlation, a coefficient matrix for the WSCC system was

calculated. As a last step, studies were done to analyze the effect of line outages on the elements of coefficient matrix. Arizona Public Service (APS) provided some possible line outages which were investigated here.

3.2 The Available Phasors

The reduced equivalent of WSCC has a total of 176 buses out of which 52 are terminals of series capacitors buses with no other injections. These bus voltages are uniquely determined by neighboring bus voltages, as explained in section 4 below. This leaves us with 124 buses where the phasors need to be estimated. The complete system has 17 PMUs installed at various substations which makes about 57 buses observable if current phasors are used. This leaves us with the task of estimating the phasors at the remaining 67 buses. However, to save time in data transmission and computation, we have assumed that only 17 positive sequence voltage phasors are available to us and the remaining 107 bus voltages need to be determined via estimation. The 17 PMU locations are as tabulated on the next page.

Table 3.1 The Available Phasors		
	1.	Malin 500-kV
BPA	2.	North 500-kV (Grand Coulee)
	3.	Montana 500-kV (Colstrip)
	4.	Big Eddy 500-kV
	5.	Midway 500-kV
PG&E	6.	Table MT 500-kV
	7.	Mossland 500-kV
	8.	Tevatr 500-kV
	9.	Fourcorn 345-kV
	10.	Navajo 500-kV
APS	11.	Paloverde 500-kV
	12.	Coronado 500-kV
	13.	Westwing 500-kV (for Pinnacle Peak 345-kV)
	14.	Adelanto 500-kV
LADWP	15.	Intermt 345-kV
	16.	Sylmarla 230-kV
	17.	Eldorado 500-kV (for McCullugh 500-kV)

The Southern California Edison system (SCE) is not included in the study report here. The Pinnacle Peak PMU was installed recently and since this bus was not in the equivalent, the Westwing 500-kV bus has been used instead. Westwing 500-kV is connected to Pinnacle Peak by a single transmission line. Similarly, it was decided earlier

that Eldorado 500-kV bus can be used to represent McCullugh 500-kV bus. The fourth PMU acquired by PG&E has not been placed yet. Therefore, for the purpose of this study, it has been assumed to be stationed at Tevatr 500-kV bus.

To get different angular patterns across the system, the whole network was divided into five smaller areas as shown in figure 4.1. The base case load and generation for each area are tabulated in Table 4.1. The total system load, generation, losses and charging MVAR are also shown. To generate a low angle profile in an area, the loads in that area were increased by some percentage and the generation in the rest of the system increased to allow power flow into that area. The loads and generations were then adjusted to get a successful power flow solution. Similarly, to raise the angles in an area compared to the rest of the system, the loads in that area were decreased and generation increased. Two areas at a time were also considered for a number of cases. The cases used for generating the coefficient matrix are listed in table 4.2. A total of 33 cases were used to generate the matrix. With 17 phasor measurements available, this gave us a redundancy factor of about 2. The results were then tested for a number of cases, some of which are shown in figures 4.2, 4.3, 4.4. Some of the test cases had load variations from bus to bus (not areawise), higher and lower load on some buses chosen randomly. This would test the matrix for situations in which the load movements are not systematic.

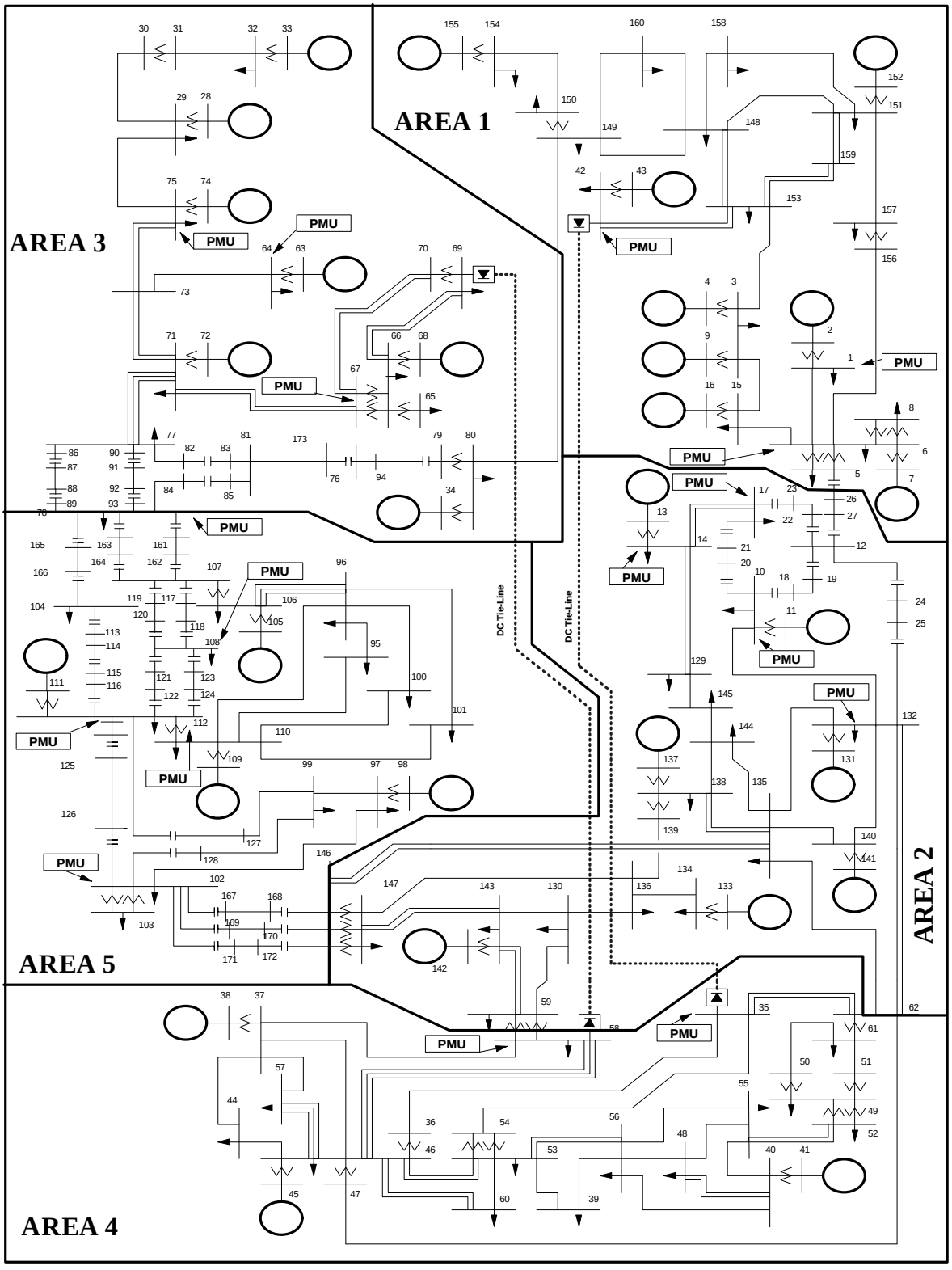

Figure 3.1 WSCC System Divided into Five Areas to Generate Various Load Flow Cases

Table 3.2 Areawise Load and Generation

AREA	Total Real Load in Area (MW)	Total Reactive Load in Area (MVAR)	Total Real Power Generation in the Area (MW)
1	9057.2	1052.2	10260.0
2	16525.3	2351.1	13317.0
3	24789.7	5264.3	28596.0
4	-1544.9	2914.5	-130.0
5	7894.11	3389.7	5378.0

Total Load	56721.41 MW	14971.75 MVAR
Total Generation	57421.00 MW	17752.31 MVAR
Losses	758.94 MW	21693.80 MVAR
Charging		15113.15 MVAR

Table 3.3 Cases Used to Generate the A-Matrix

Case No.	Area/Areas where load was changed	New Load in this area (% of base case)	Case No.	Area/Areas where load was changed	New Load in this area (% of base case)
1.	1	80	18.	3, 4	90
2.	2	80	19.	3, 5	90
3.	3	90	20.	4, 5	80
4.	4	75	21.	1, 2	110
5.	5	80	22.	1, 3	110
6.	1	110	23.	1, 4	110
7.	2	105	24.	1, 5	110
8.	3	110	25.	2, 3	110
9.	4	110	26.	2, 4	110
10.	5	110	27.	2, 5	110
11.	1, 2	90	28.	3, 4	110
12.	1, 3	90	29.	3, 5	110
13.	1, 4	90	30.	4, 5	110
14.	1, 5	80	31.	1,2,3,4,5	90
15.	2, 3	90	32.	1,2,3,4,5	105
16.	2, 4	80	33.	None	(base case)
17.	2, 5	80			

Table 3.4 Description of Test Cases Used as Examples

Test Case No.	Description
1.	About ±10% change in loads at randomly selected buses (about 30 buses in total)
2.	Area 1 - 90% of base load
3.	Area 2 - 90% of base load
4.	Area 3 - 95% of base load
5.	Area 4 - 90% of base load
6.	Area 5 - 90% of base load
7.	Areas 1 and 2 - 110% of base load and Areas 3 and 5 - 90% of base load
8.	Areas 1 and 2 - 90% of base load and Areas 3 and 5 - 110% of base load

3.3 Mathematical Formulation

Let x be a vector of measured magnitude (or angles) at the 17 PMU buses, and let y be a vector of unmeasured magnitudes (or angles) at the remaining 107 buses.

x = [17 x 1] measured quantities

y = [107 x 1] unmeasured quantities

Let A be an unknown connection matrix which links the two vectors x and y.

A = [107 x 17]

We then have the postulated relationship

$$[\,y\,]_{(107x1)} = [\,A\,]_{(107x17)} \text{ x } [\,x\,]_{(17x1)} \tag{3.1}$$

Using the 33 simulated load flow results, we have 33 sets of y and x. Hence, for 33 cases:

$$[\,y\,]_{(107x33)} = [\,A\,]_{(107x17)} \text{ x } [\,x\,]_{(17x33)} \tag{3.2}$$

$$[\,y\,]^{T}_{(33x107)} = [\,x\,]^{T}_{(33x17)} \text{ x } [\,A\,]^{T}_{(17x107)} \tag{3.3}$$

$$[\,A\,]^{T}_{(17x107)} = [\,x\,]^{T}_{(33x17)} \setminus [\,y\,]^{T}_{(33x107)} \text{ (in MATLAB terms)} \tag{3.4}$$

This gives the least square approximation. The actual formula would be:

$$[\,A\,]^{T} = ([\,x\,][\,x\,]^{T})^{-1} [\,x\,][\,y\,]^{T} \tag{3.5}$$

After having obtained $[\,A\,]$, the unknown phasors can be calculated using equation 3.1. The voltage magnitudes and angles are decoupled and hence each has one coefficient matrix. The same equations hold for both magnitudes and angles.

Having estimated **A**, the next task is to test if the matrix **A** can be used to determine the unknown vector **y** for a set of measured phasors **x** in a new load flow case. To verify this,

tests were performed using the cases listed in table 3.3. The parameters estimated with the proposed **A** matrix were then compared with the actual parameters in these cases. The results for each of these cases are shown as graphs in the next section. In these graphs the dotted line is the estimated parameter while the solid line is the actual parameter. In case of electronic PDF files, the blue colored line is the estimated parameter while the red one is actual. The difference between the estimate and the actual is the error introduced by this procedure and is shown as error plots.

3.4 Estimation Results on Sample Cases

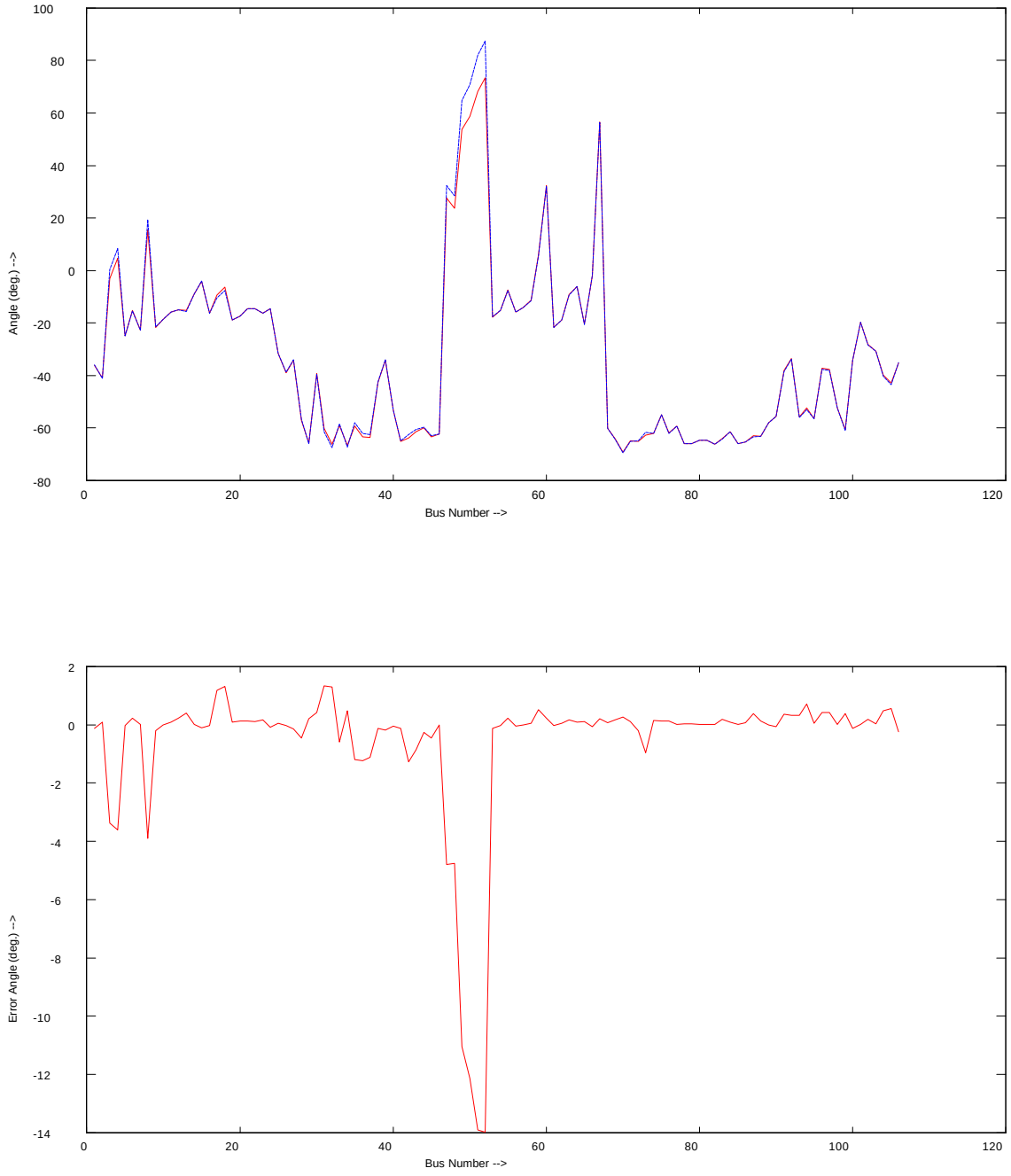

Figure 3.2 Test Case 1 - Angles

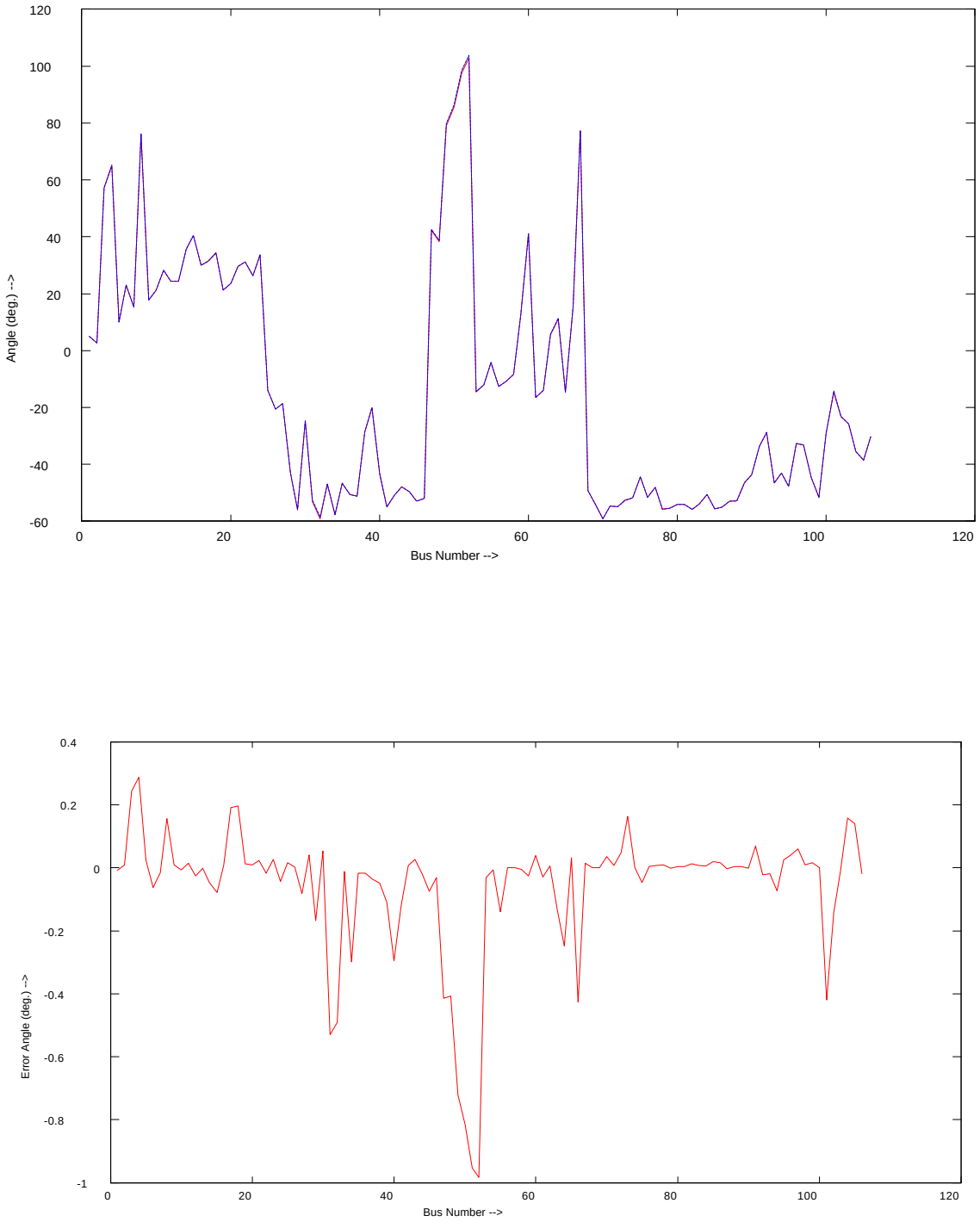

Figure 3.3 Test Case 2 - Angles

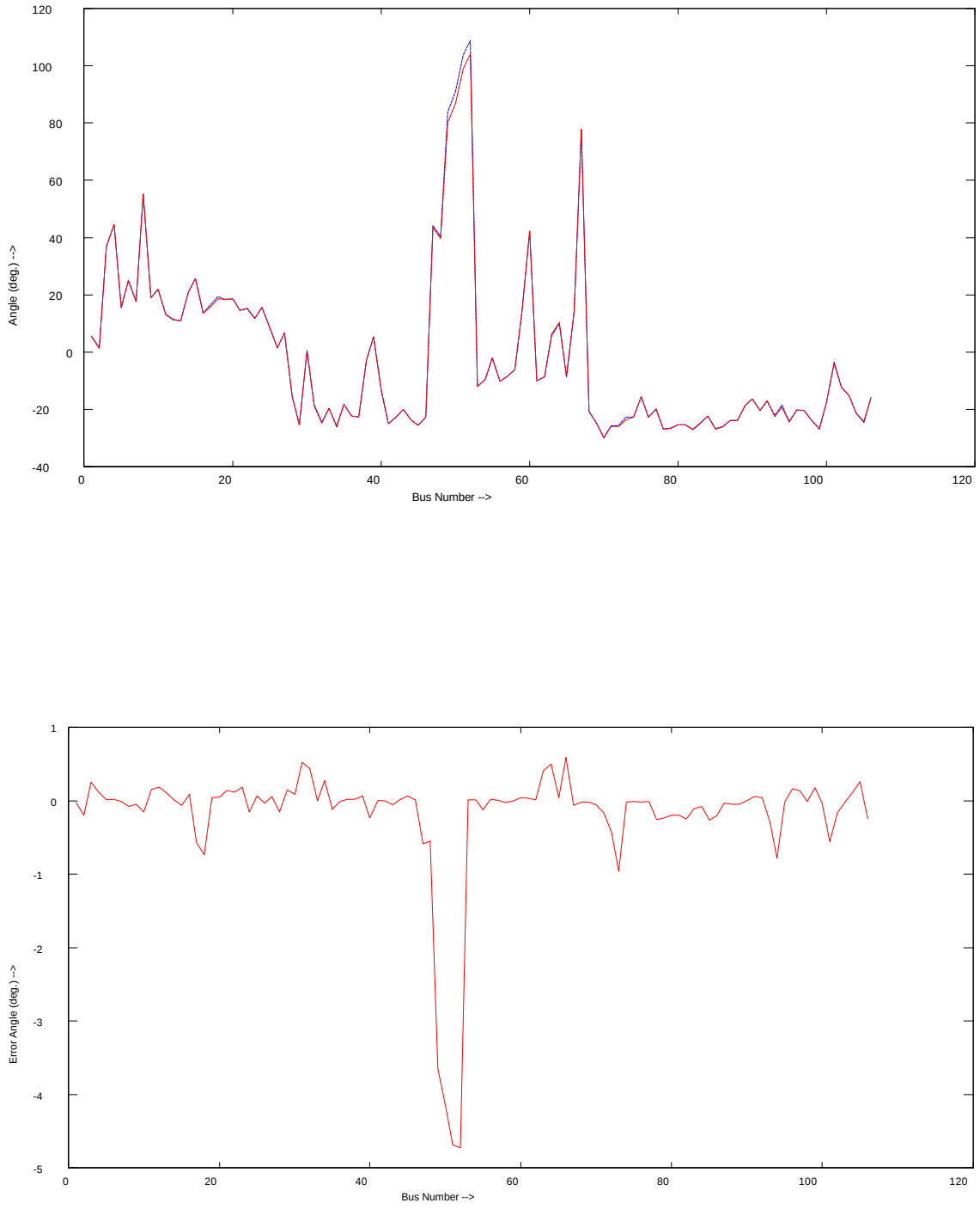

Figure 3.4 Test Case 3 - Angles

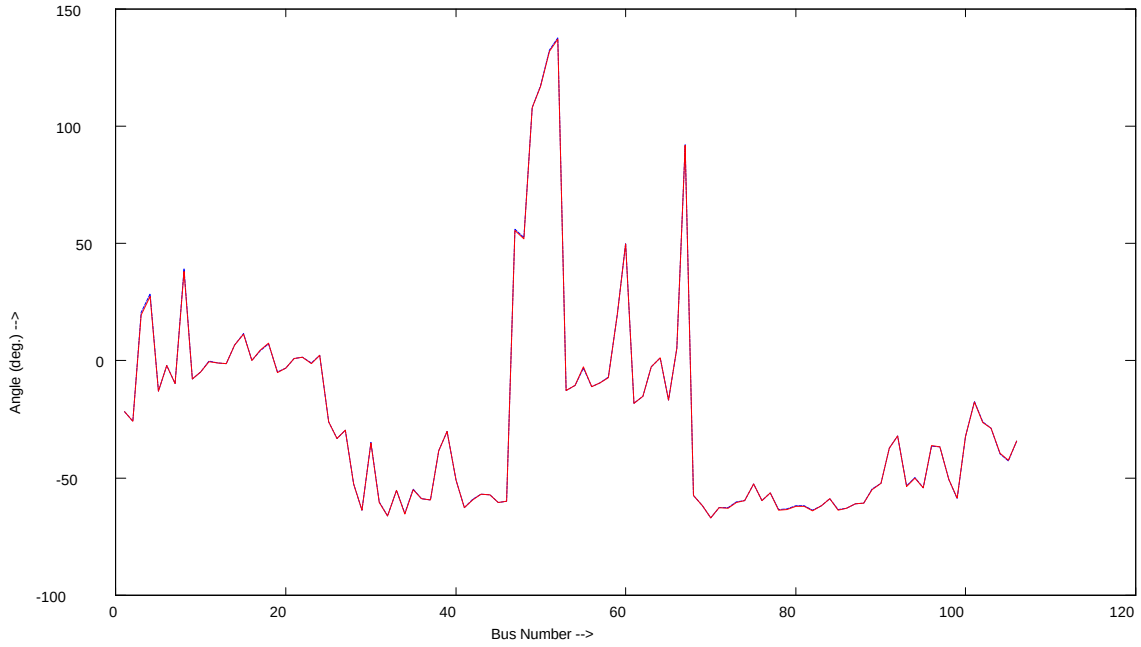

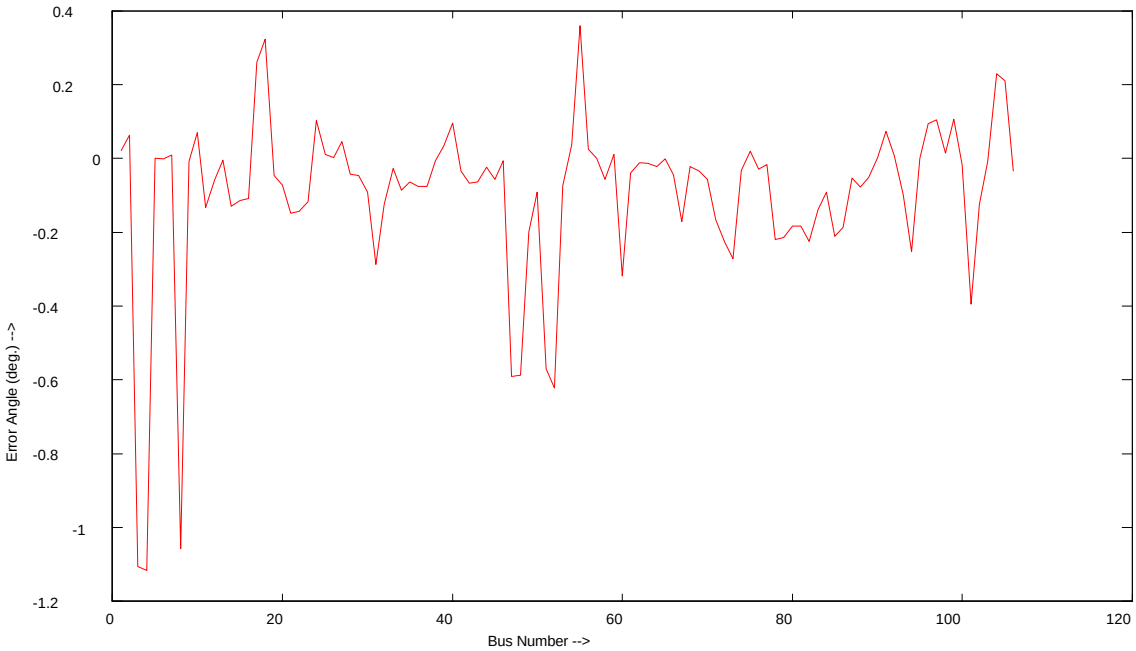

Figure 3.5 Test Case 4 - Angles

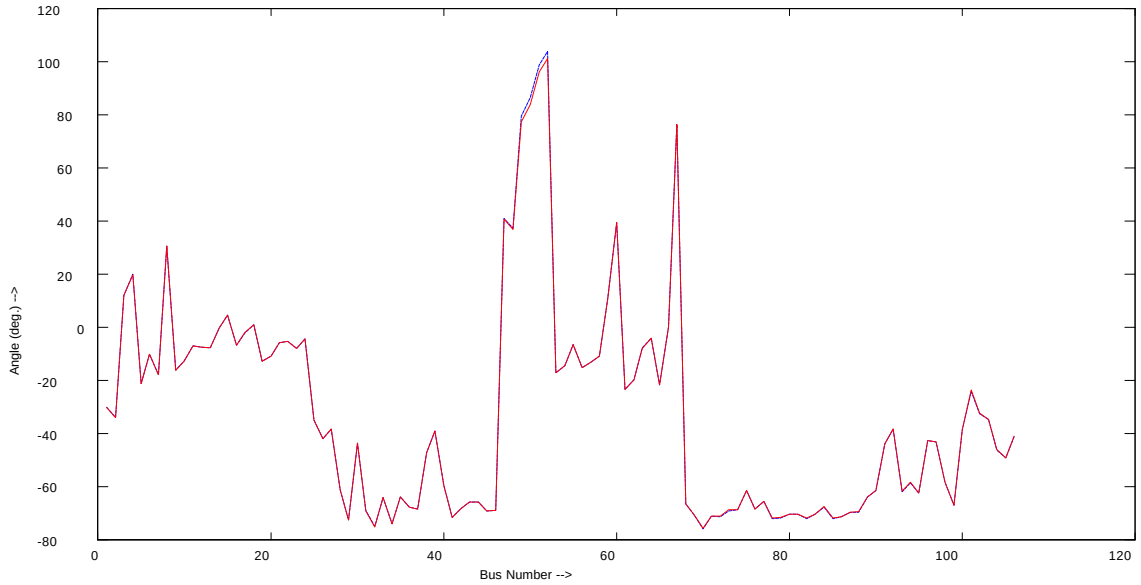

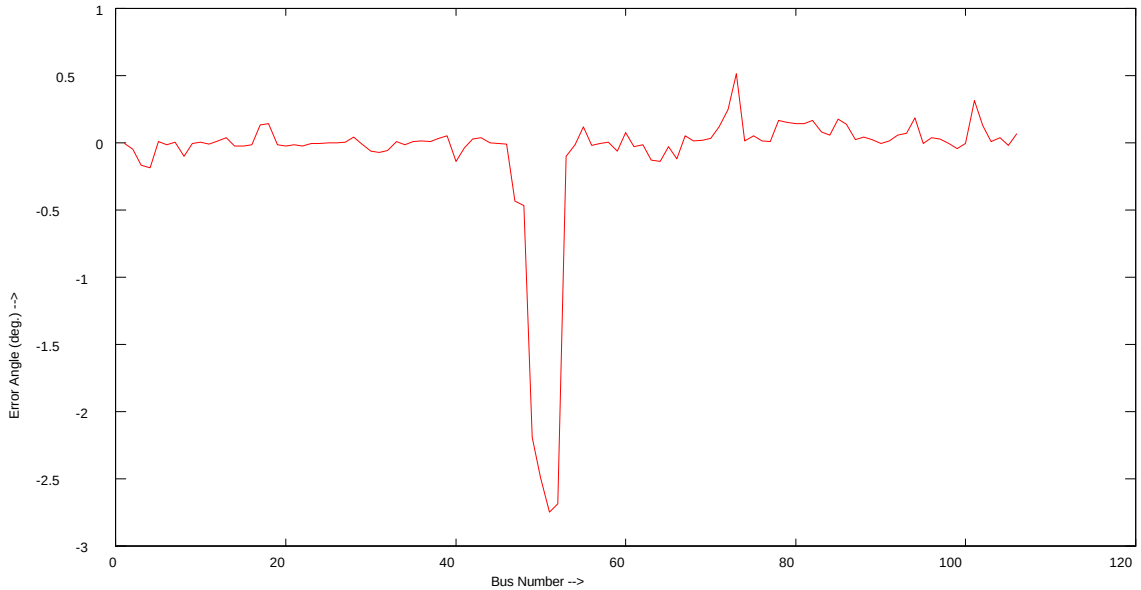

Figure 3.6 Test Case 5 - Angles

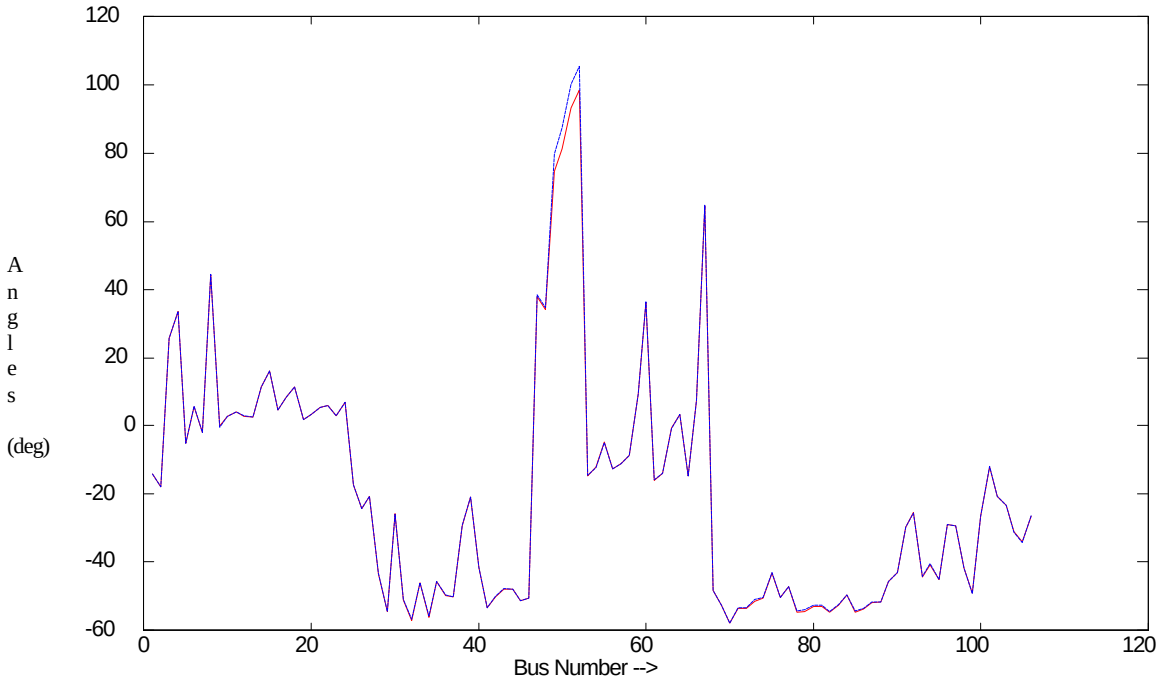

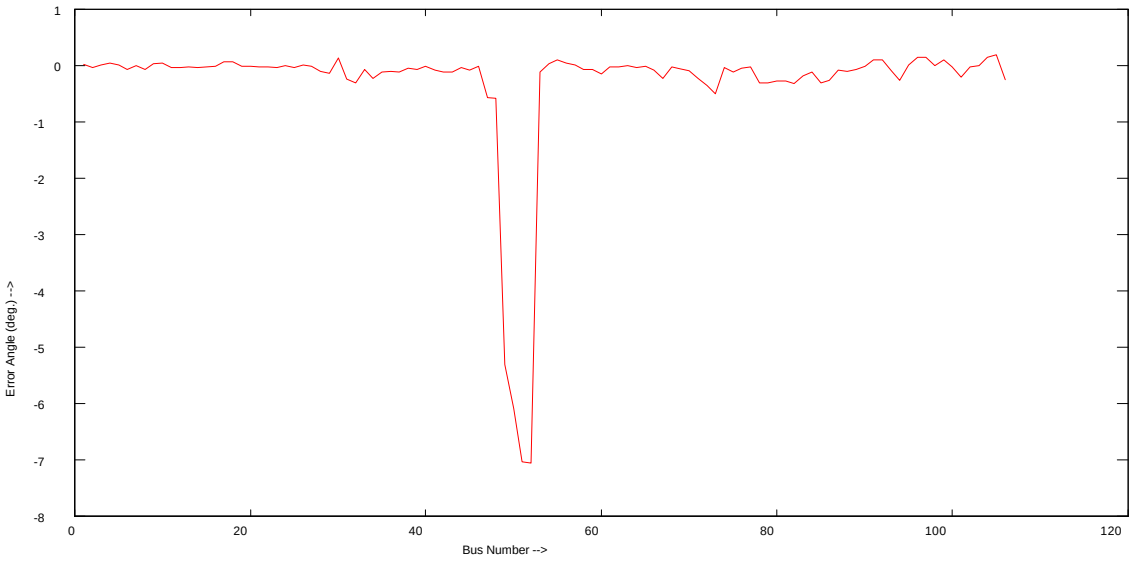

Figure 3.7 Test Case 6 - Angles

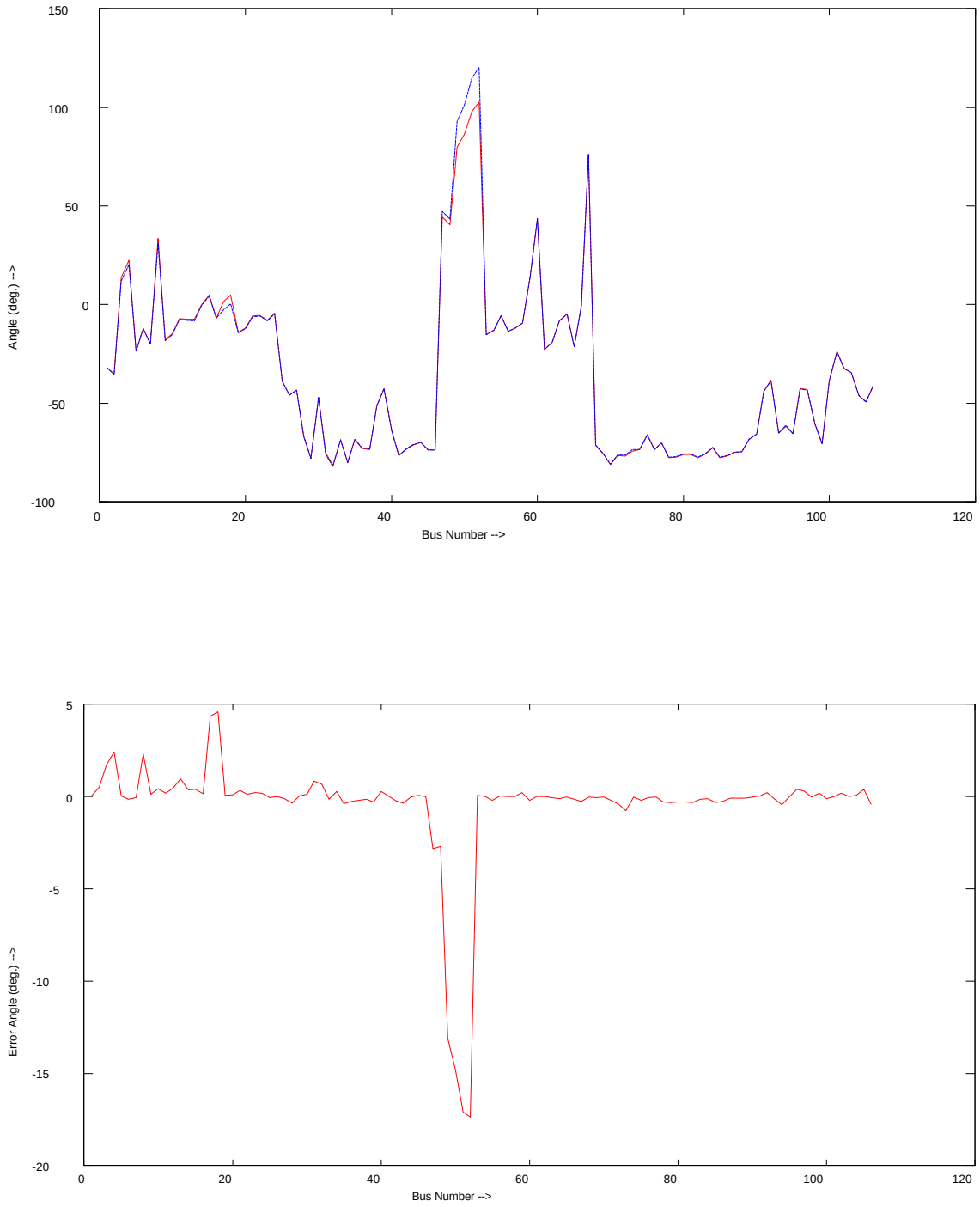

Figure 3.8 Test Case 7 - Angles

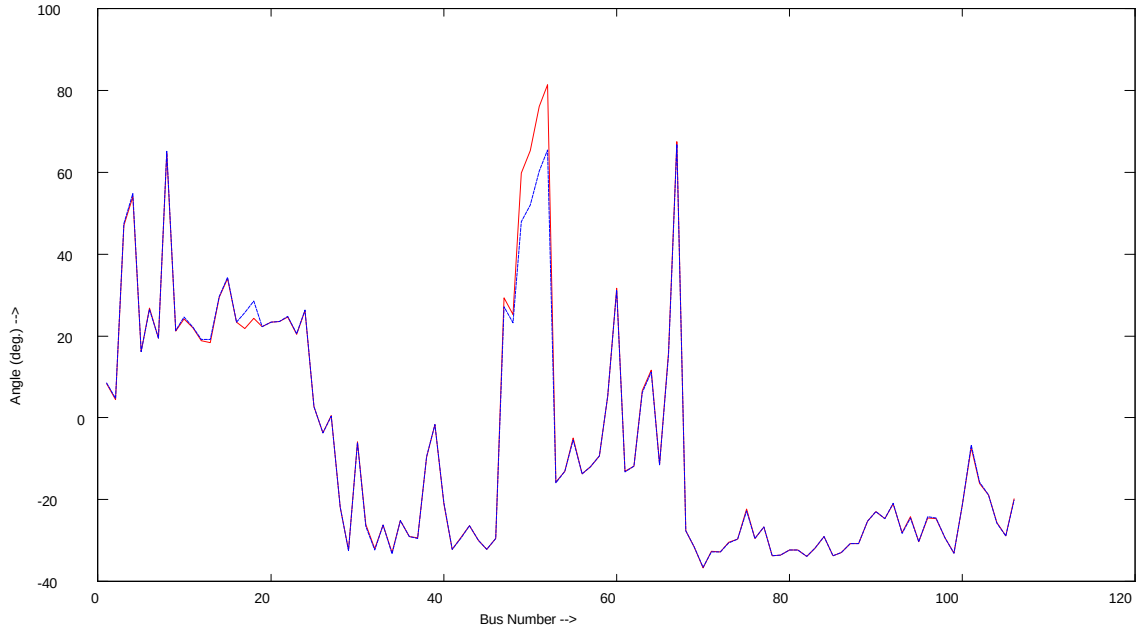

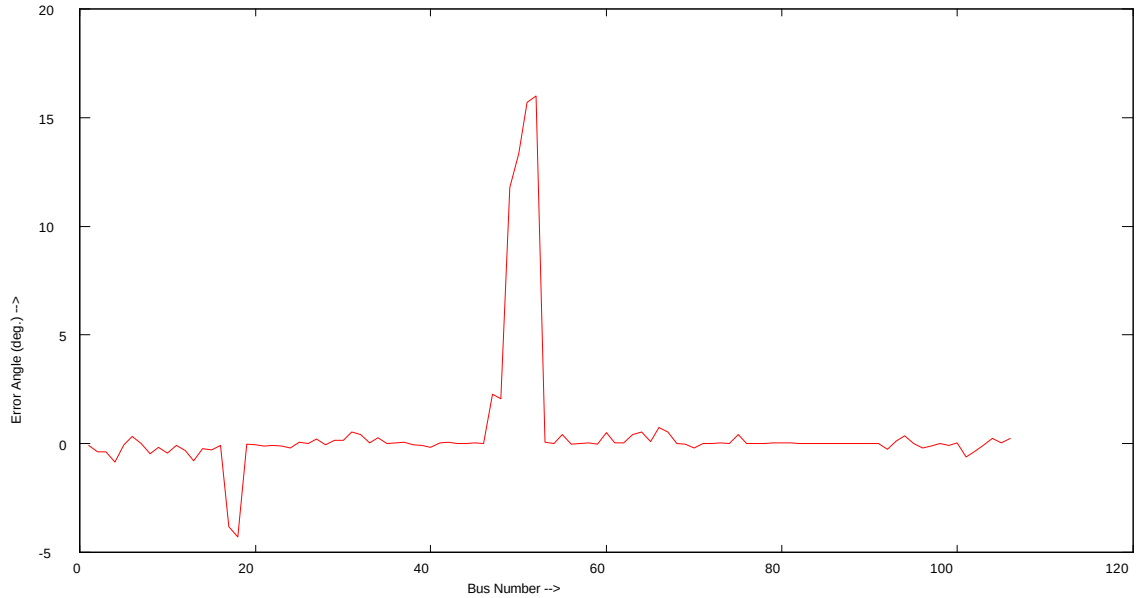

Figure 3.9 Test Case 8 - Angles

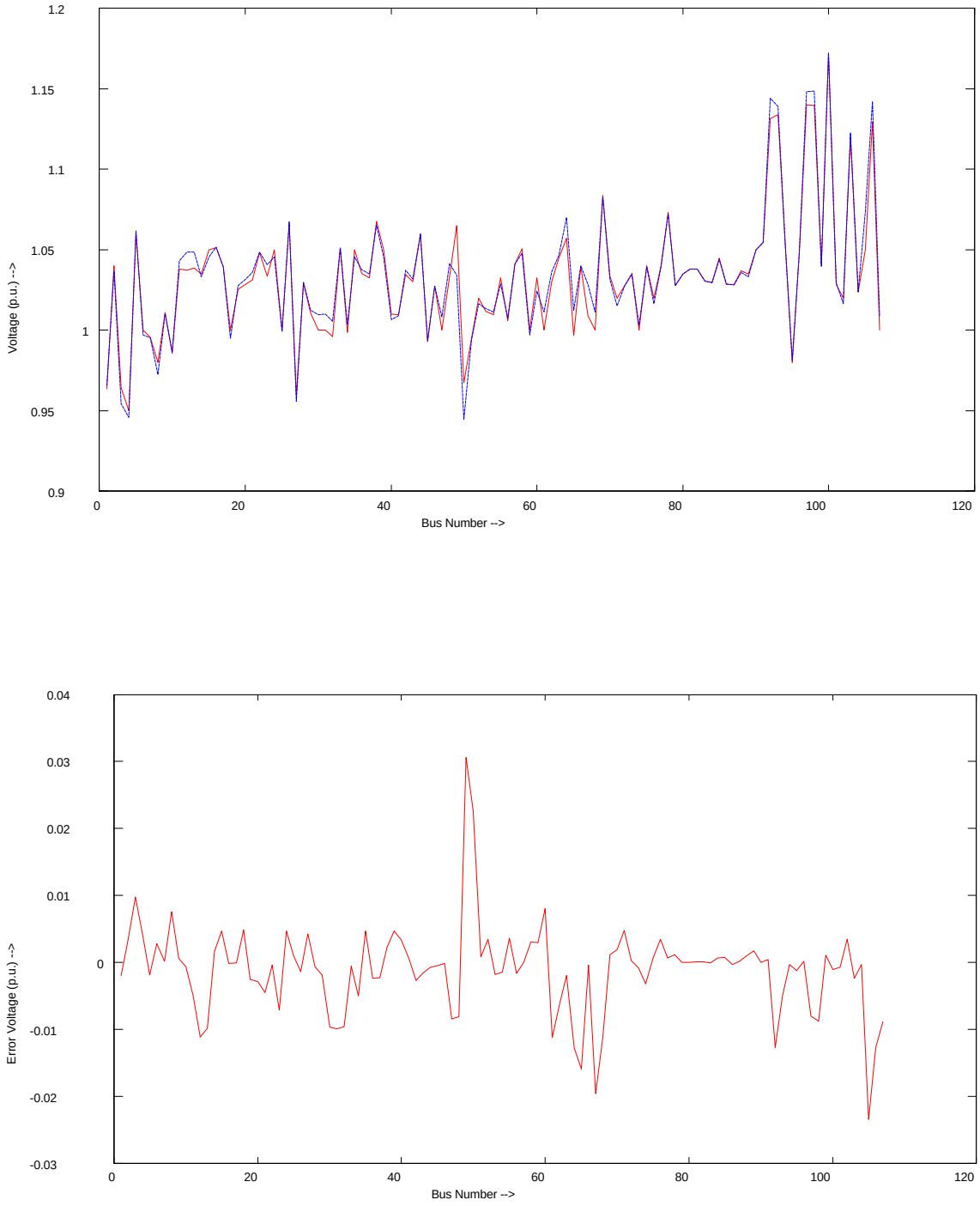

Figure 3.10 Test Case 1 - Voltages

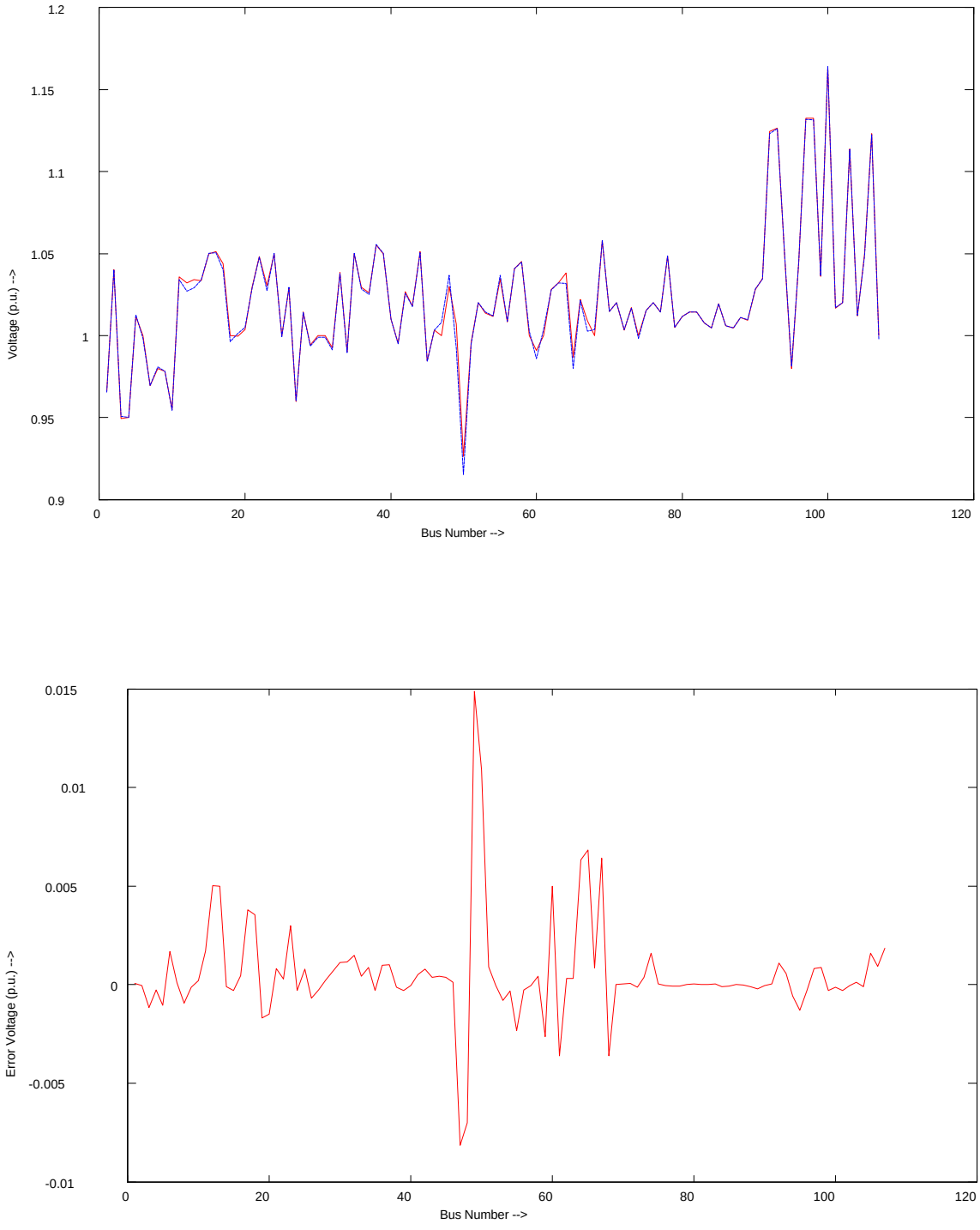

Figure 3.11 Test Case 2 - Voltages

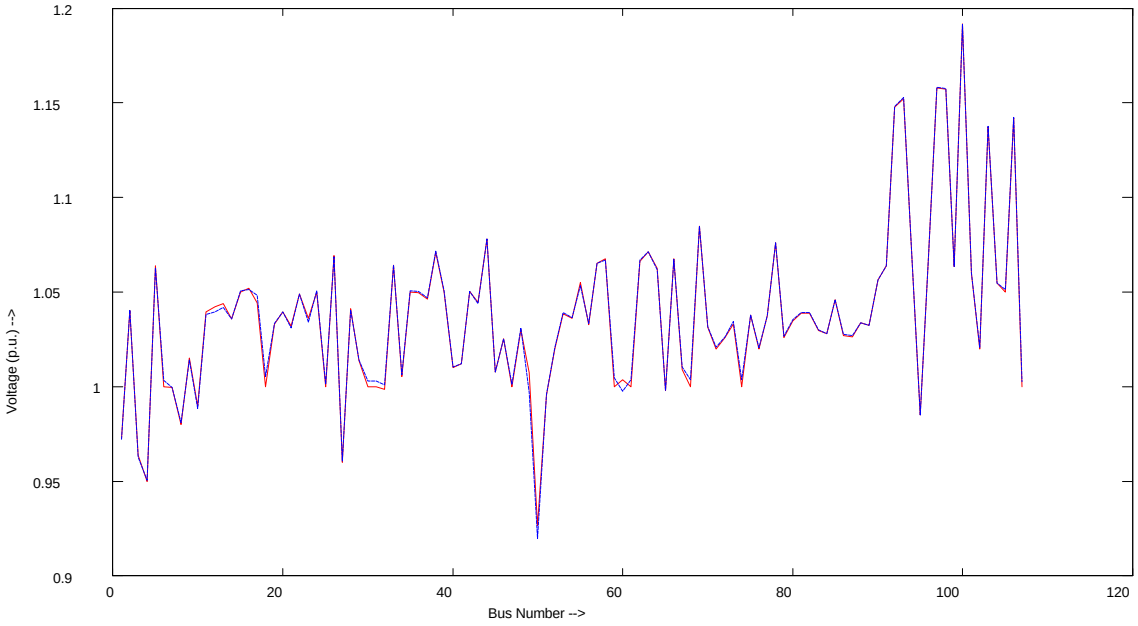

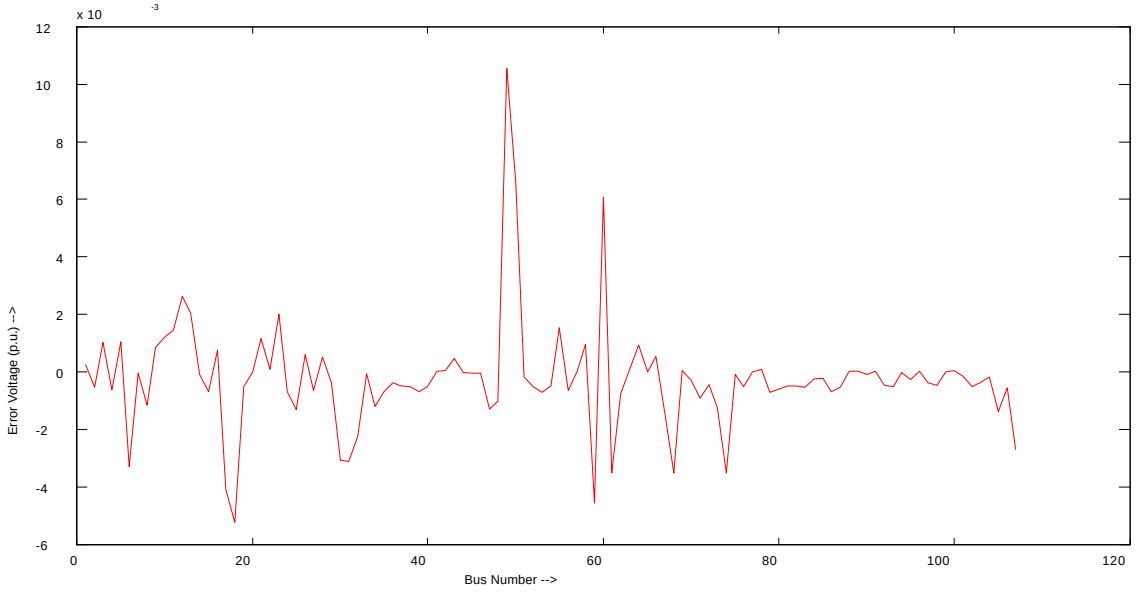

Figure 3.12 Test Case 3 - Voltages

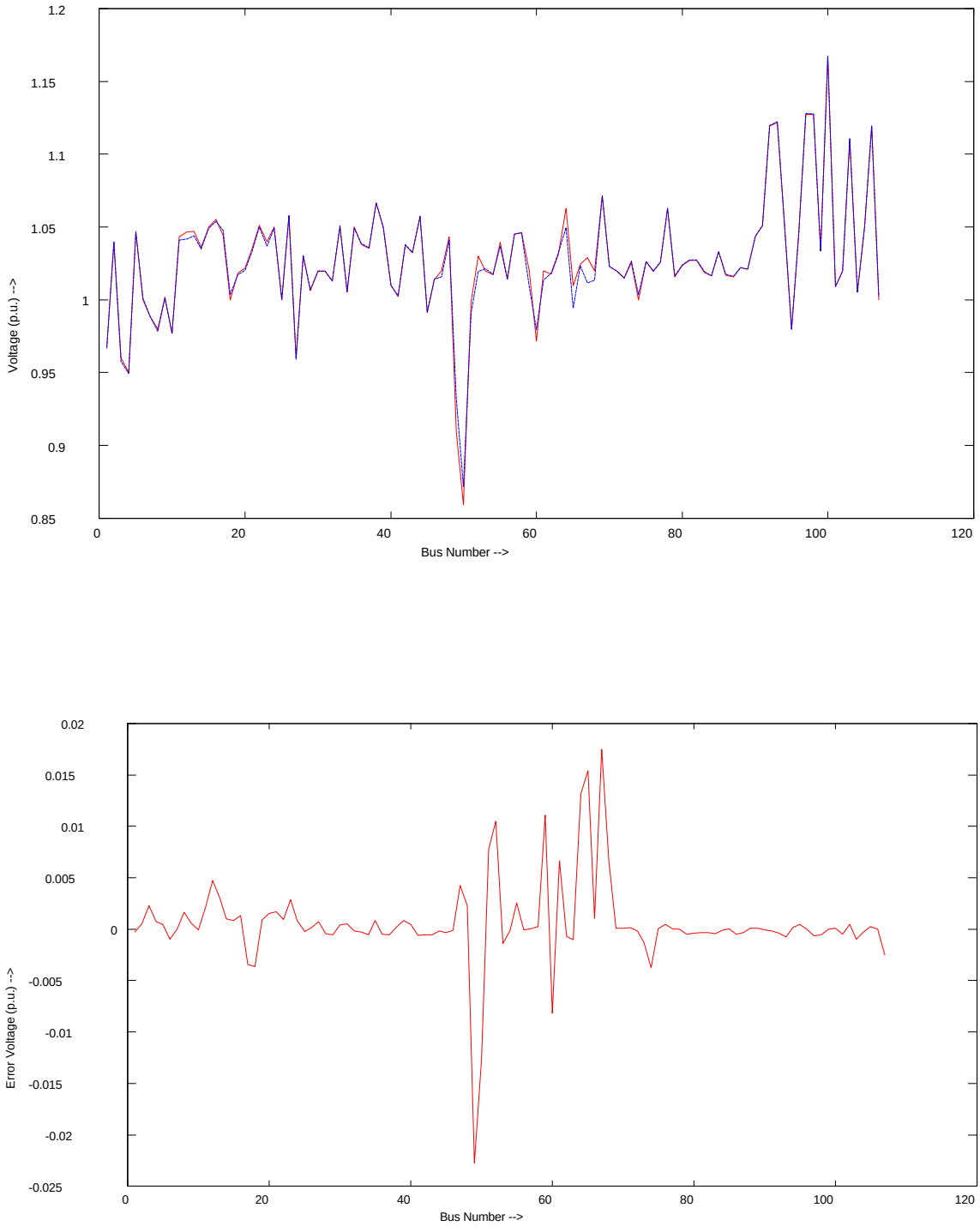

Figure 3.13 Test Case 4 - Voltages

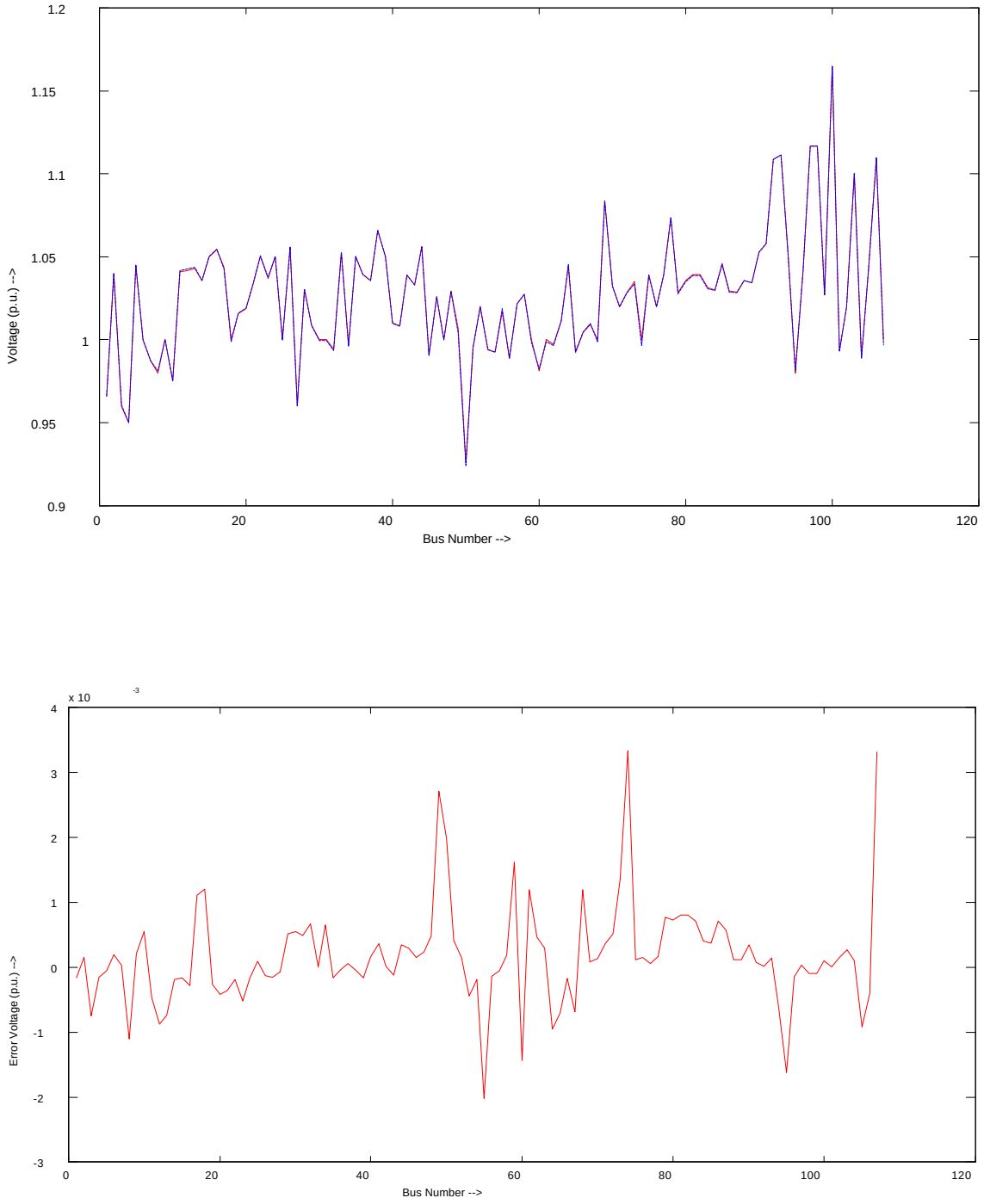

Figure 3.14 Test Case 5 - Voltages

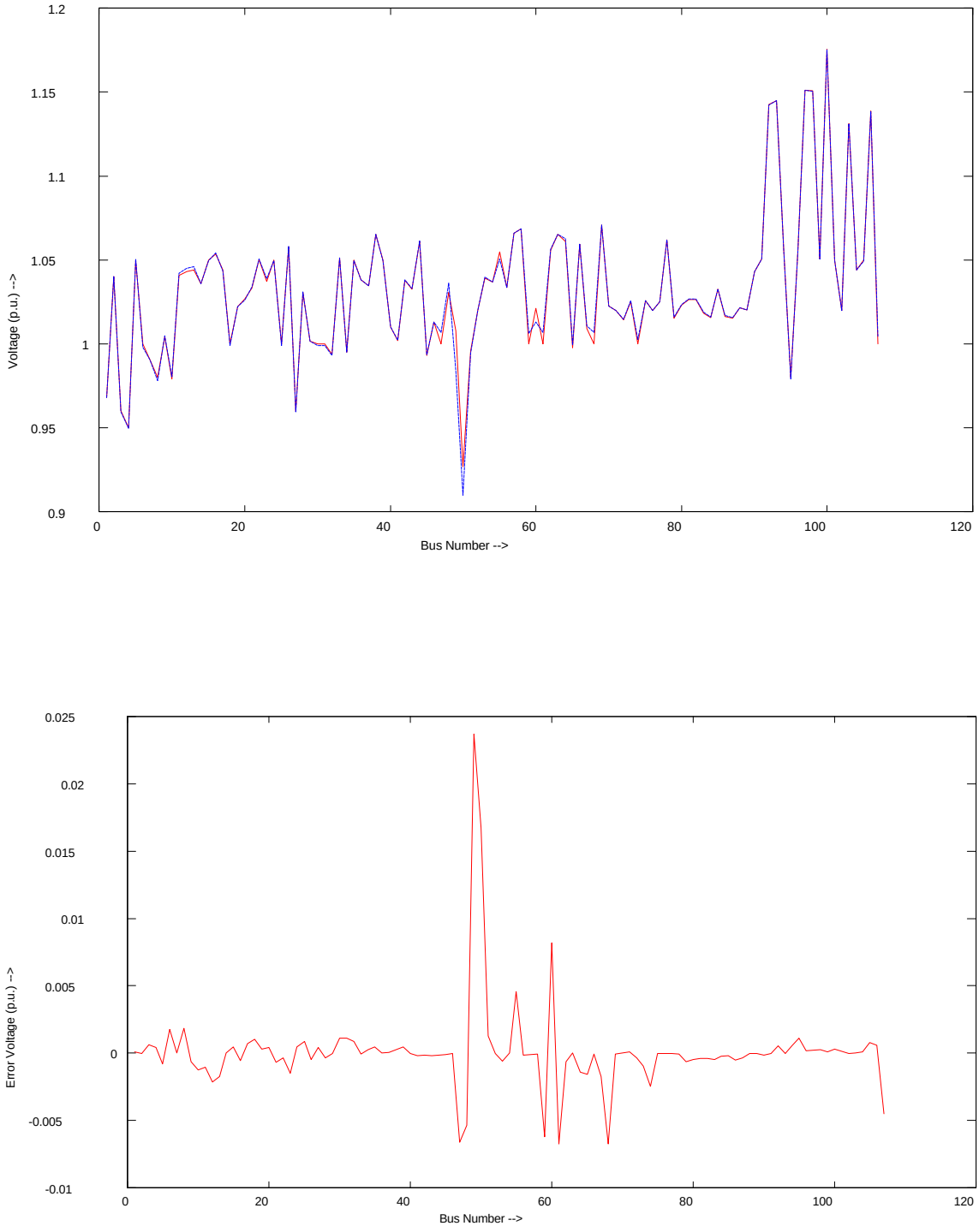

Figure 3.15 Test Case 6 - Voltages

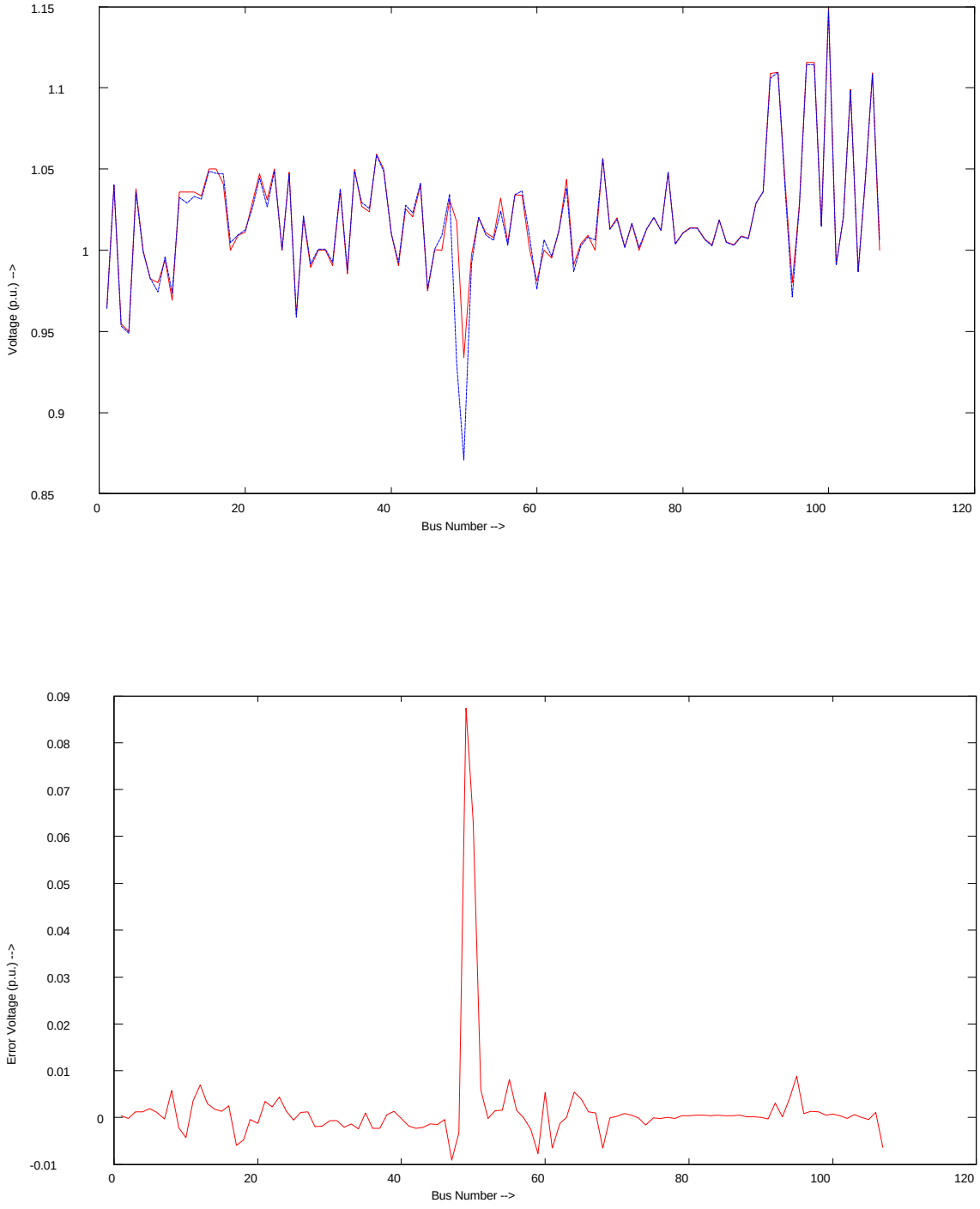

Figure 3.16 Test Case 7 - Voltages

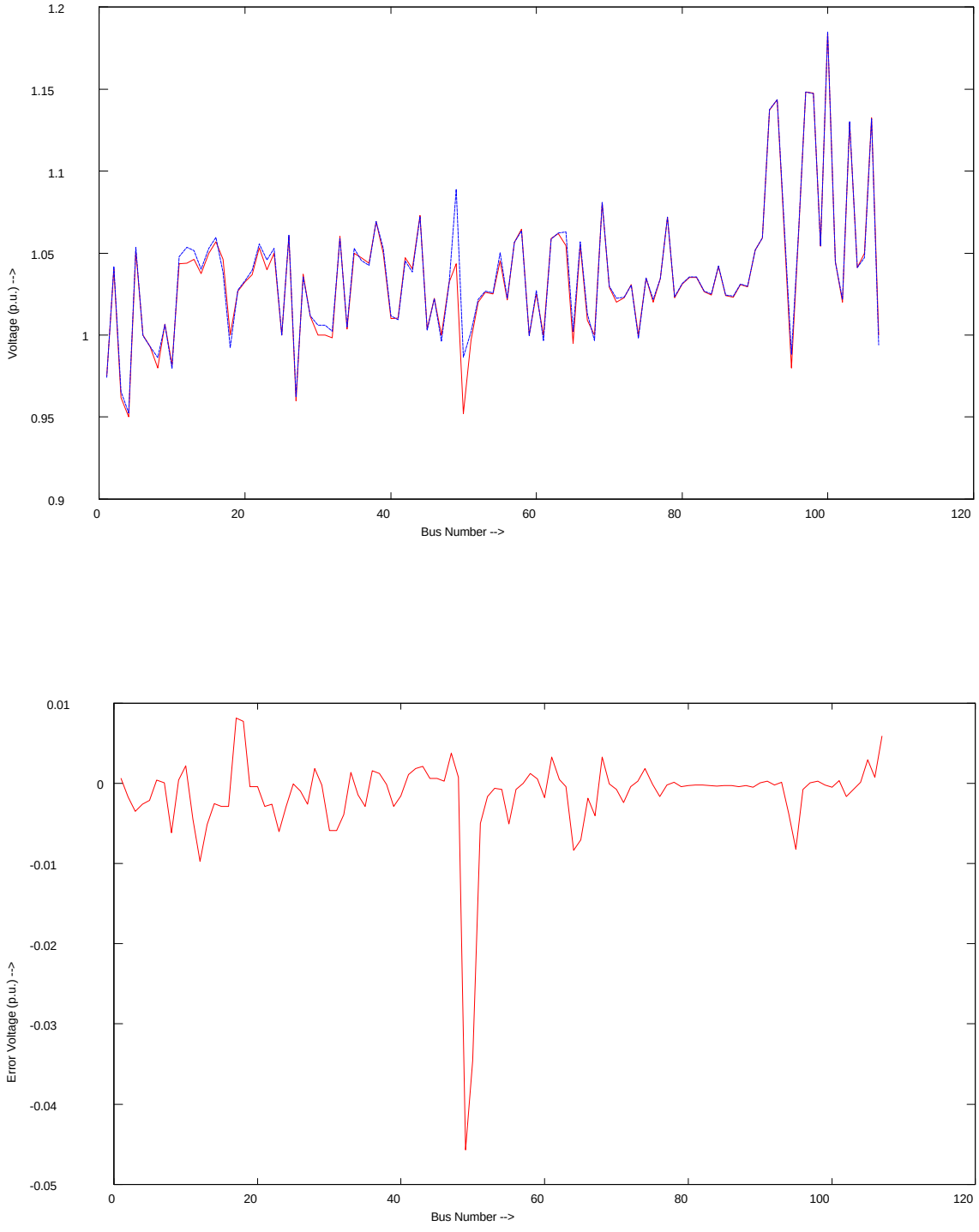

Figure 3.17 Test Case 8 - Voltages

The results of the estimation of angles and voltages in the eight cases illustrated above were very satisfactory. The errors at most buses were limited to ±4 degrees in angles and ±0.02 p.u. in voltages with the exception of four buses. These four buses belong to Canada region and a distinct behavior in the case of these buses could be a result of absence of PMUs in the region. Also, it was felt that the representation of the system by a 173 bus equivalent was not sufficient at certain points in the system.

On a closer look at the results, the errors seem to be pronounced at the same buses in all test cases. An effort to identify these buses reveals that some of the erroneous buses are:

1. Craig 22.0
2. Hayden 20.0
3. Midpoint 345
4. Bridger2 22
5. Round MT 20.0
6. Naughton 230.

On identifying the exact locations of these buses it has been found that all these buses are at least 3 buses away from a PMU site, with the exception of Round MT which is only two buses away from a PMU site. However, another significant point to notice is that four of these six buses are generation sites and the other two (Midpoint 345 and Naughton 230) are directly connected to generating stations (Bridger2 22 and Naught 20.0 respectively). This might lead to two conclusions. First, that the further away a bus is from a PMU, the worse is estimation at this bus. Secondly, sudden load changes at load buses close to a generation site without an adjustment in generation causes the angles at generation sites to change drastically in the resulting load flow solution while the change at load buses is absorbed by the inertia of a heavy load. In reality however, a change in load at a bus close to a generation site will cause some change in generation to meet the extra demand or absorb the loss in demand. In these simulations, when load scenarios were created, the generation close to buses with a load change was not changed. This was done to create various angle patterns.

3.5 Line Outage Studies

The suitability of the coefficient matrix in case of line outages was tested by simulating line outages and then using the same coefficient matrix to estimate the parameters. The success of this test would indicate that the coefficient matrix is a rigid correlation between the phasors at various buses and thus absorbs the effects of any lineoutages. To simulate line outages, lines were removed from the network data and to accomodate for the lost power transfer on the line, loads and generations were dropped on the appropriate sides of the line. Line Outage Studies were done for the following cases supplied by Arizona Public Service Company (APS):

1. Moenkopi - Four Corners 500 kV line
2. Moenkopi - Eldorado 500 kV line
3. Moenkopi - Navajo 500 kV line
4. Palo Verde - Devers 500 kV lines # 1 & 2
5. Palo Verde - West Wing 500 kV line
6. Four Corners - Cholla 345 kV lines # 1 & 2

Studies could not be done for the Palo Verde - San Diego 500 kV line because of its absence in the 176 bus equivalent. The results of the studies are summarized in the following graphs. It is again noted that the results are fairly satisfactory eith the exception of some buses in the Canada region. These are the same buses that had a large error margin even in the normal load flow cases. It further consolidates the conclusion that measurement in this region is not sufficient. This also makes case for a larger number of PMUs. As the number of PMUs grow, the estimations from such a coefficient matrix would be more accurate. However, the error margins in case of line outages have considerably increased. In most cases, errors in angles are limited to ±20 degrees and voltage errors are limited to ±0.06 p.u.. In the case of Paloverde-Westwing 500 kV line outage, the voltage error is more than 0.3 p.u at 3 buses.

3.6 Results of Line Outage Studies

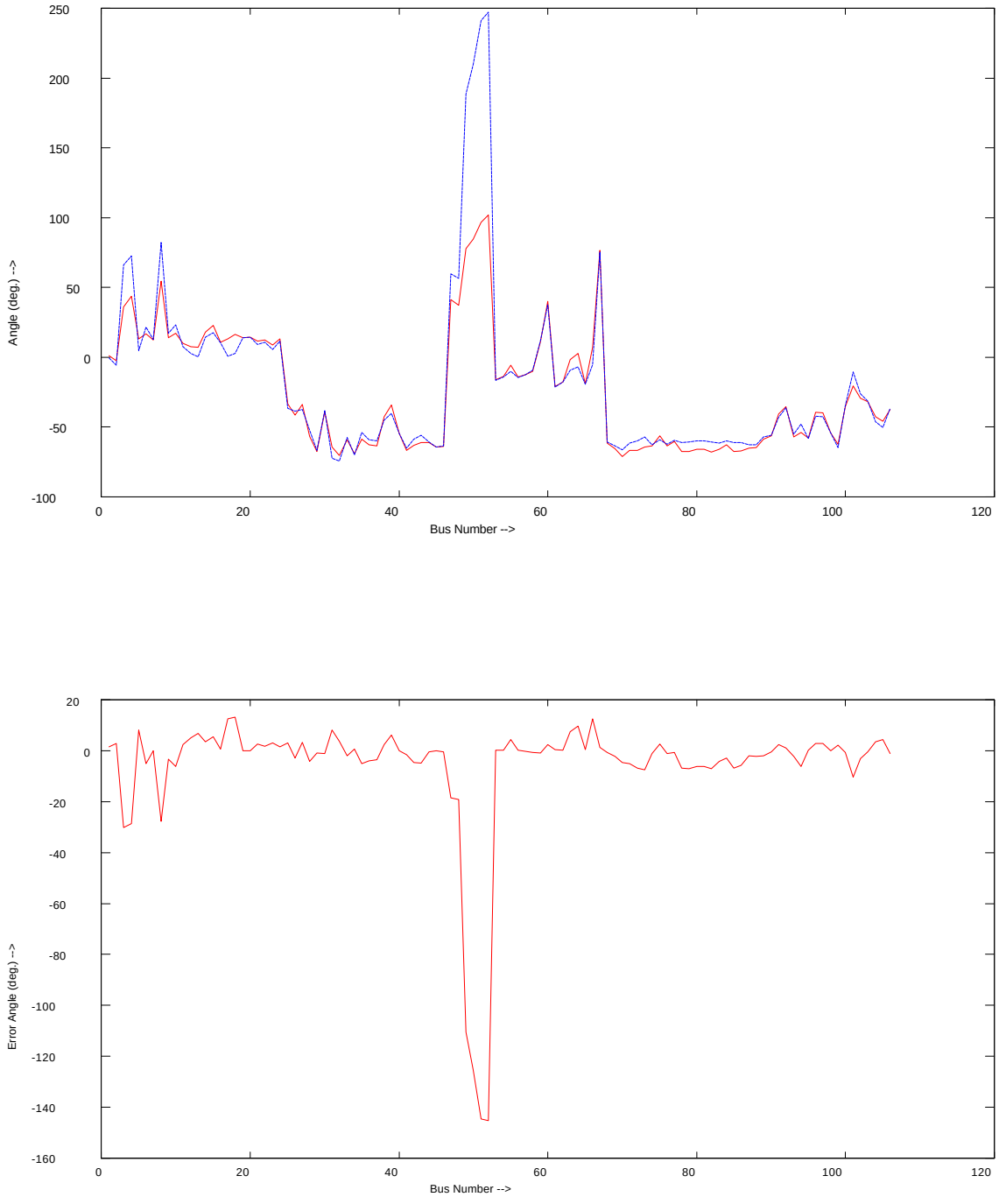

Figure 3.18 Line Outage Case 1 - Angles

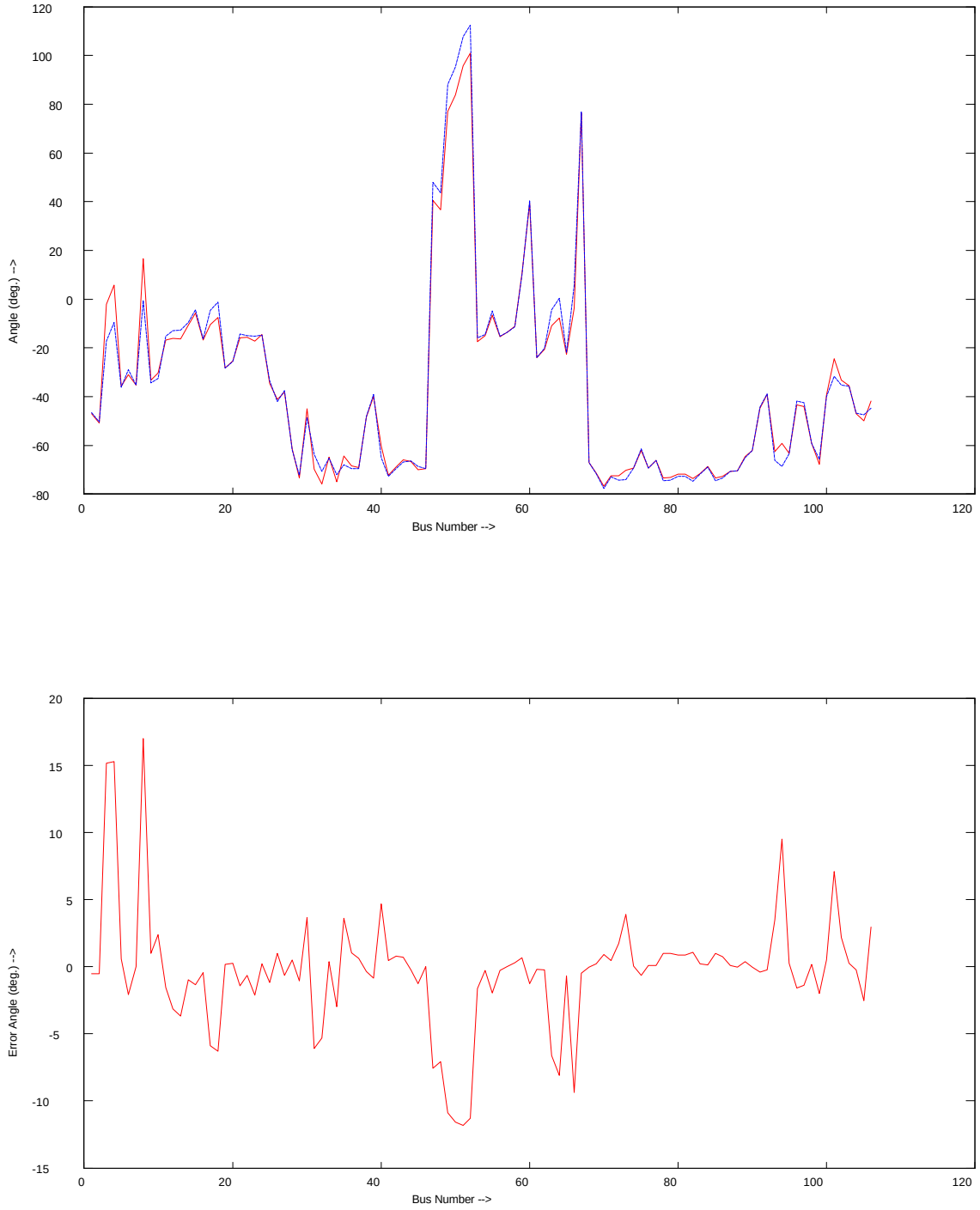

Figure 3.19 Line Outage Case 2 - Angles

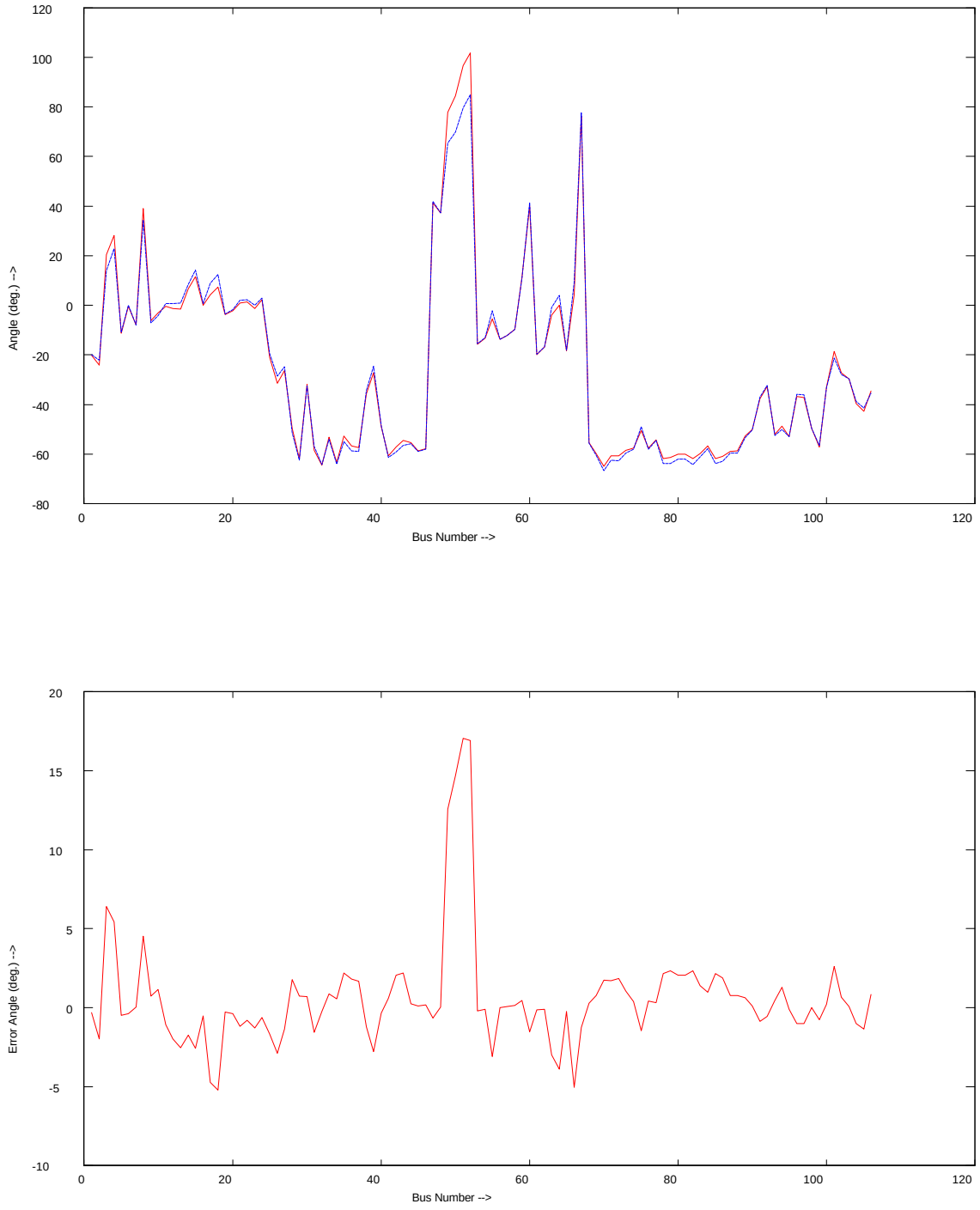

Figure 3.20 Line Outage Case 3 - Angles

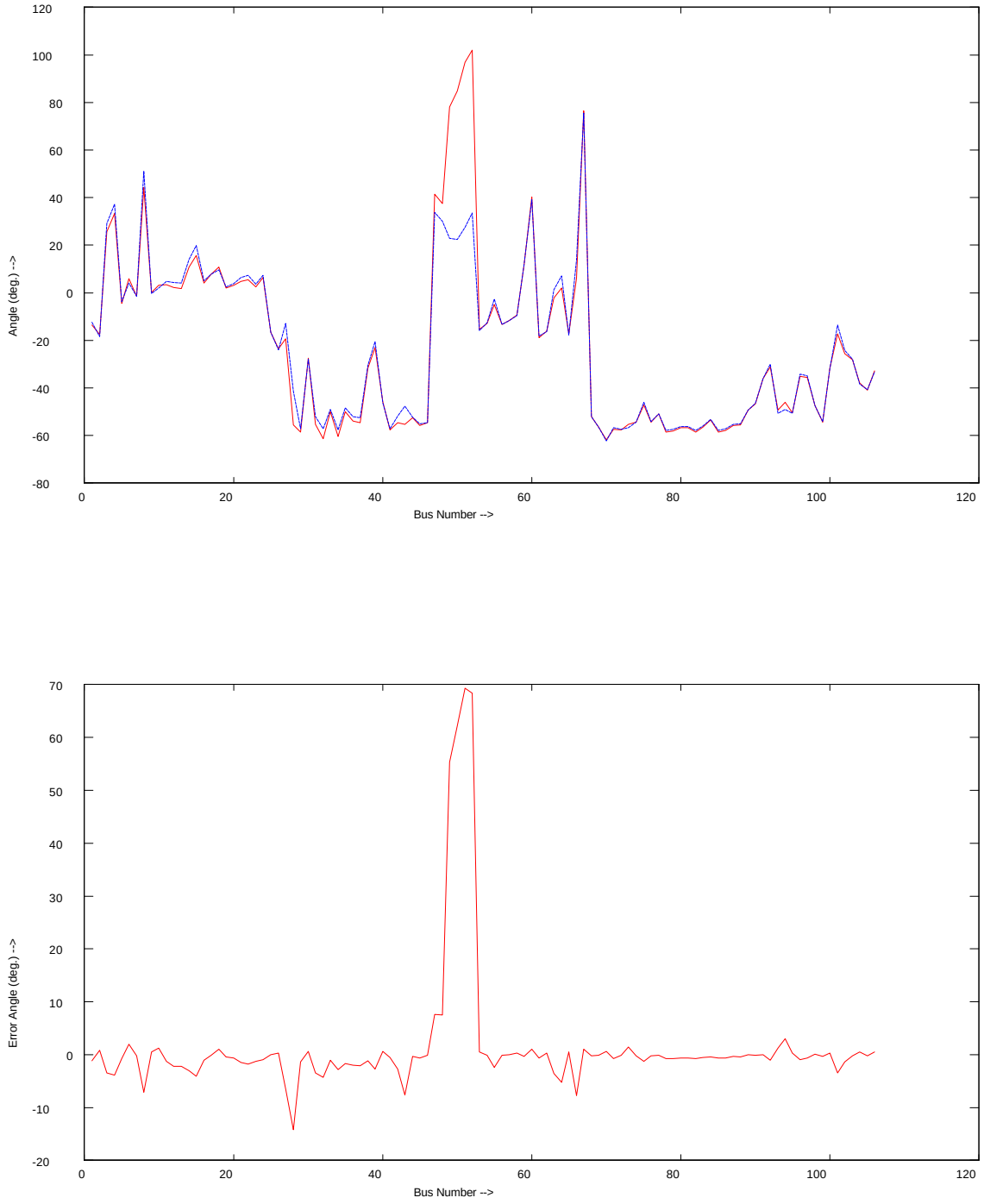

Figure 3.21 Line Outage Case 4 - Angles

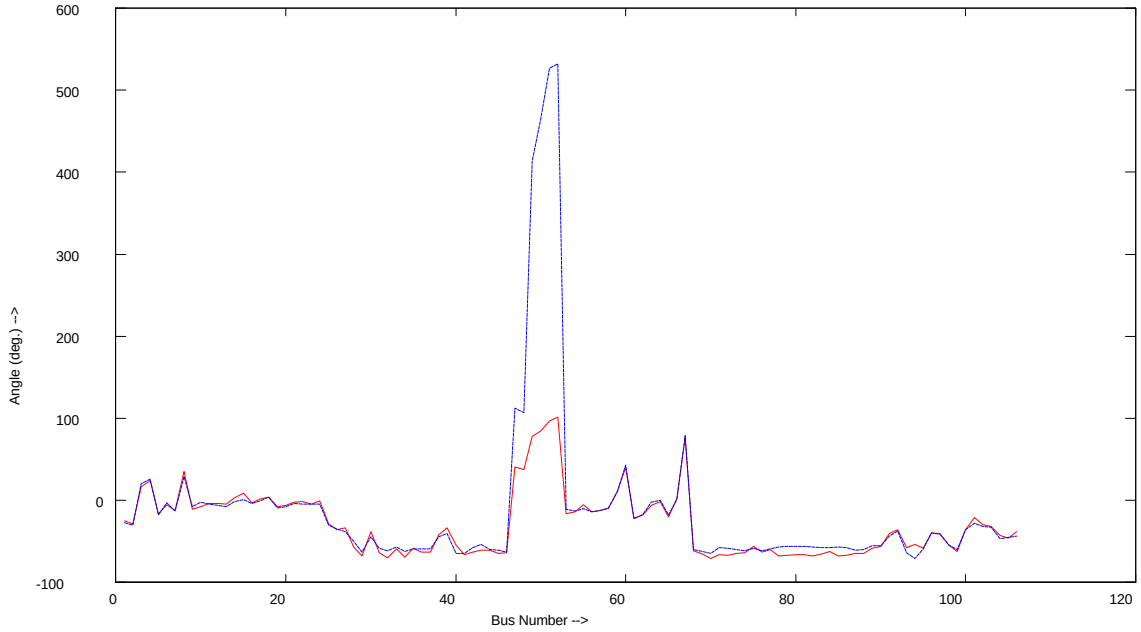

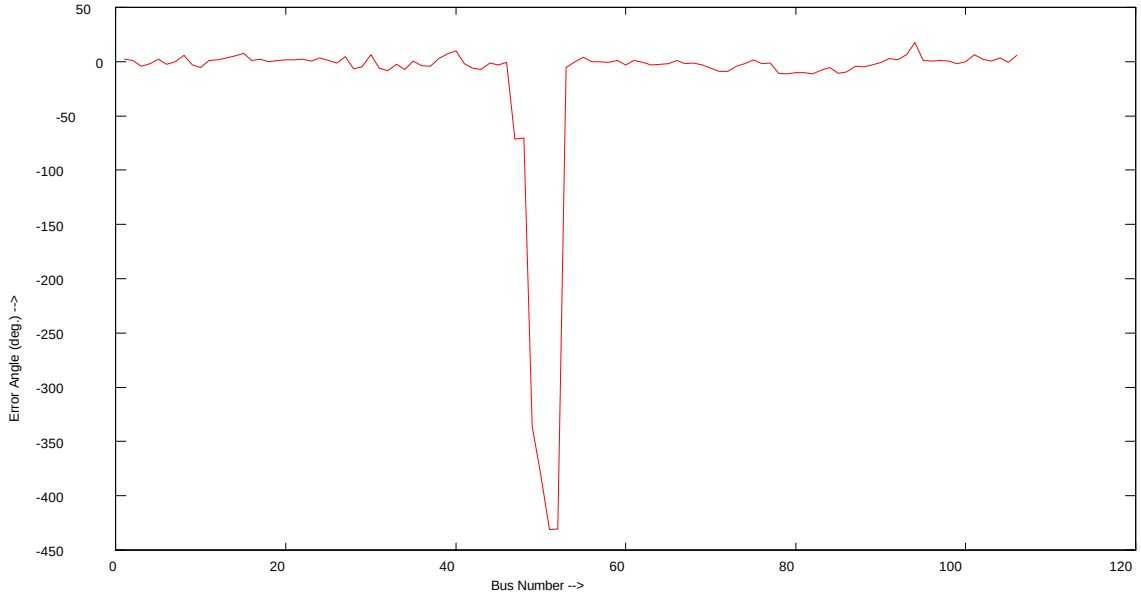

Figure 3.22 Line Outage Case 5 - Angles

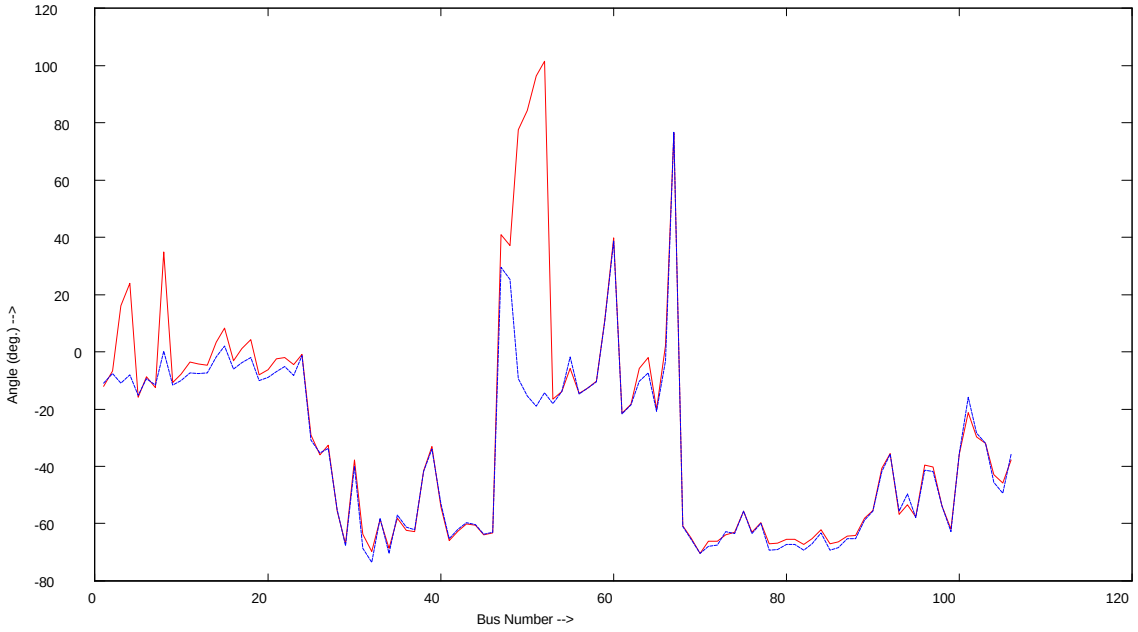

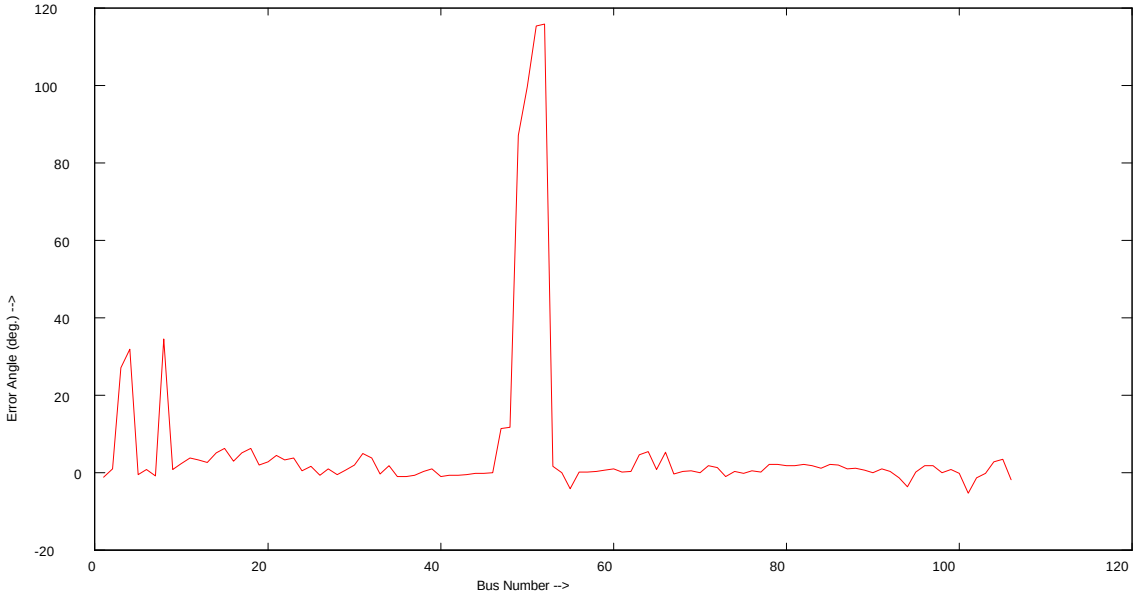

Figure 3.23 Line Outage Case 6 - Angles

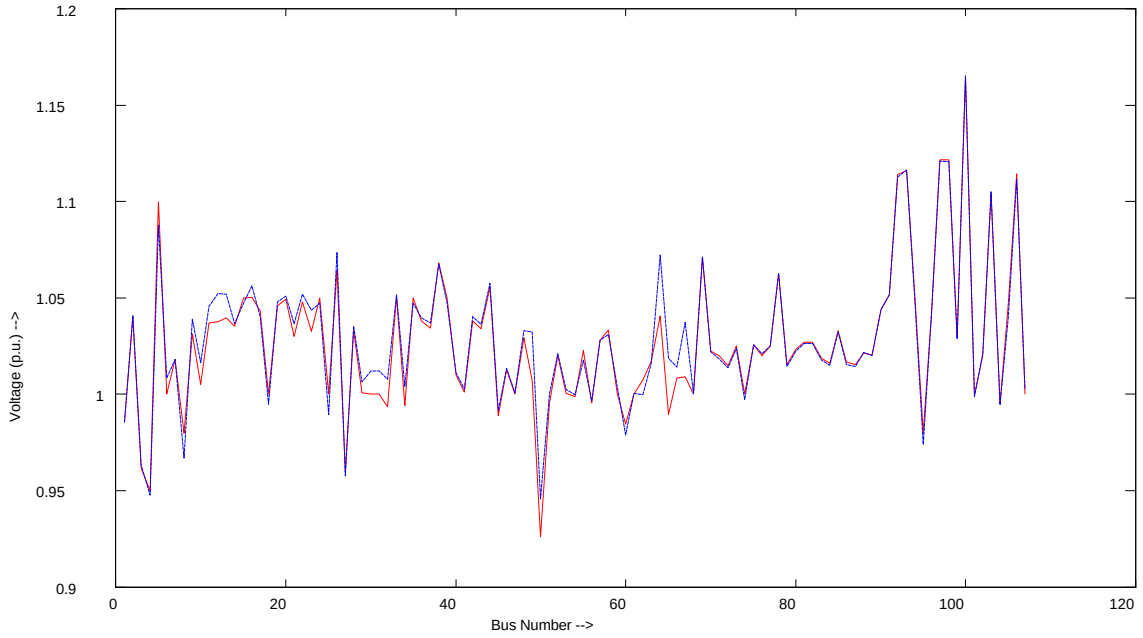

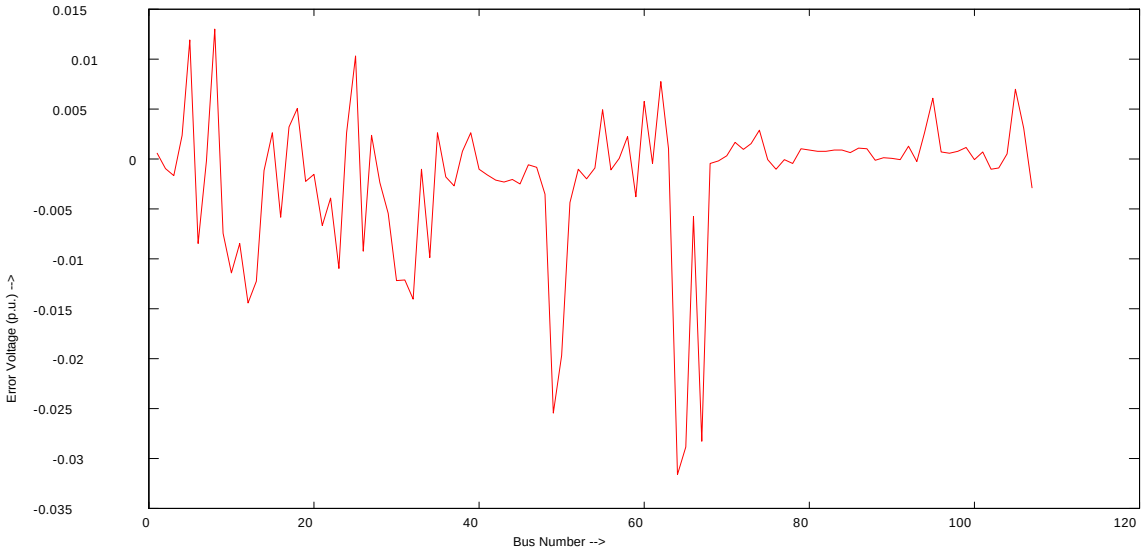

Figure 3.24 Line Outage Case 1 - Voltages

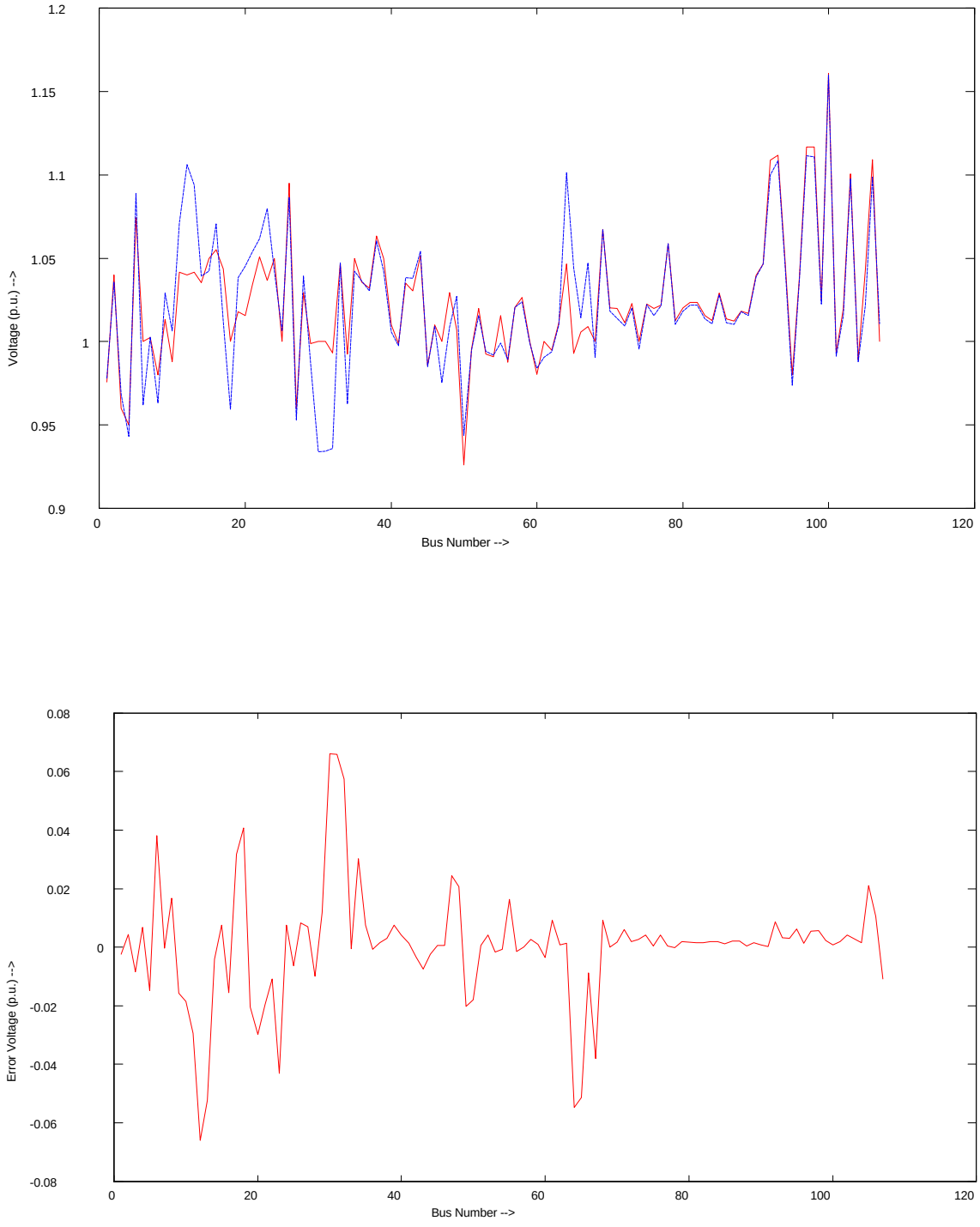

Figure 3.25 Line Outage Case 2 - Voltages

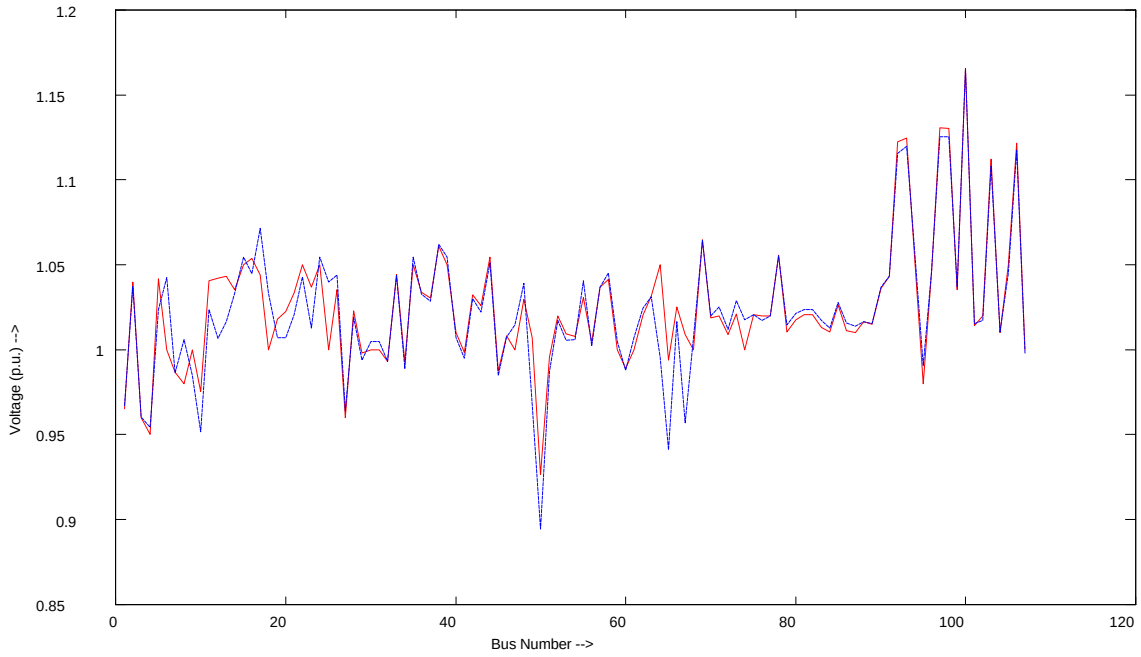

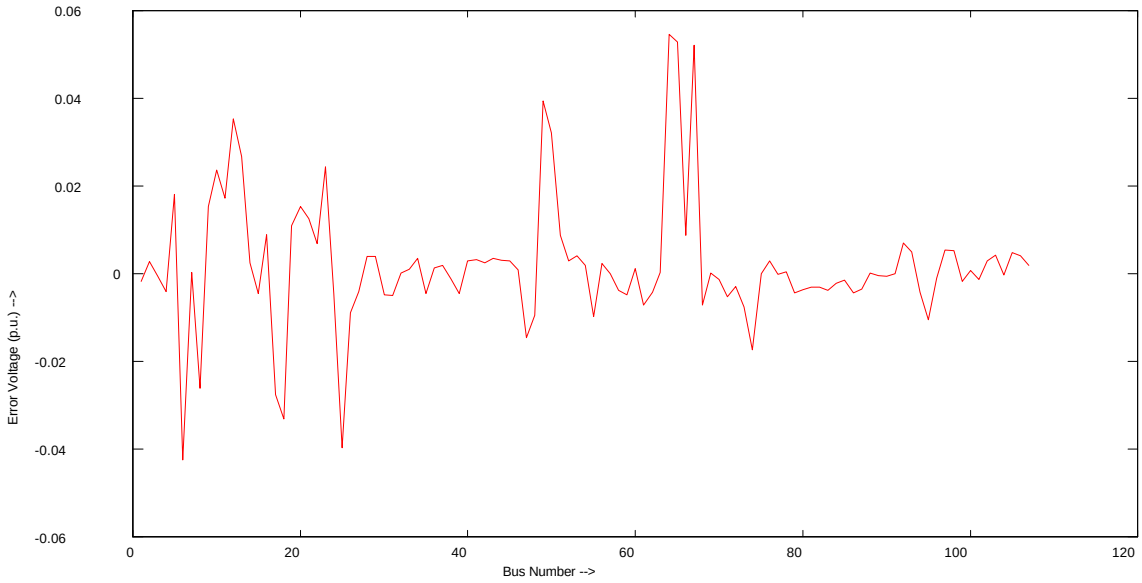

Figure 3.26 Line Outage Case 3 - Voltages

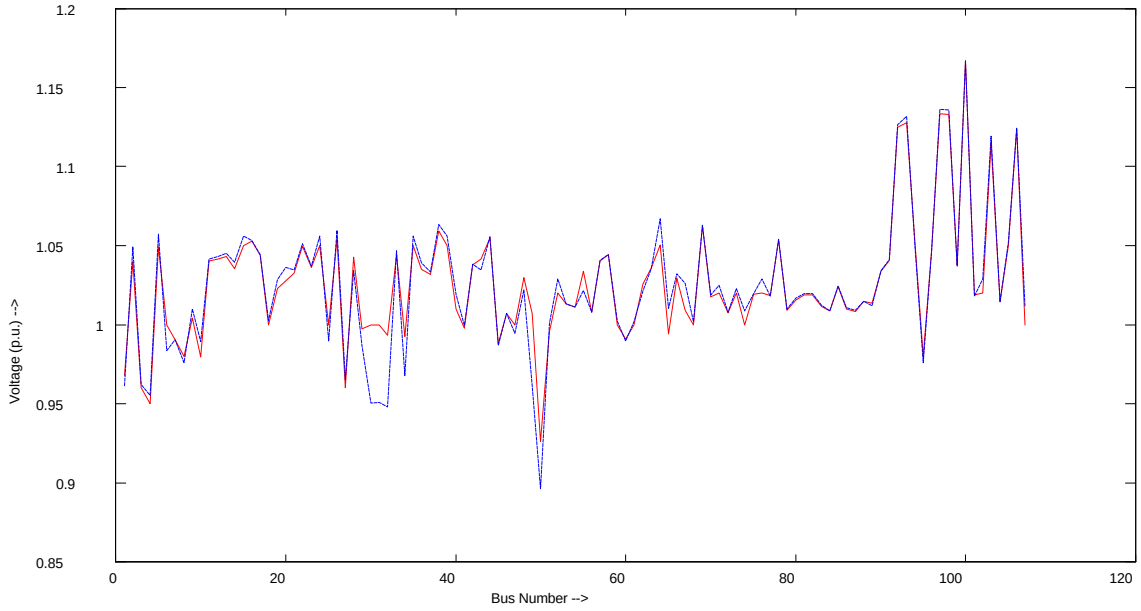

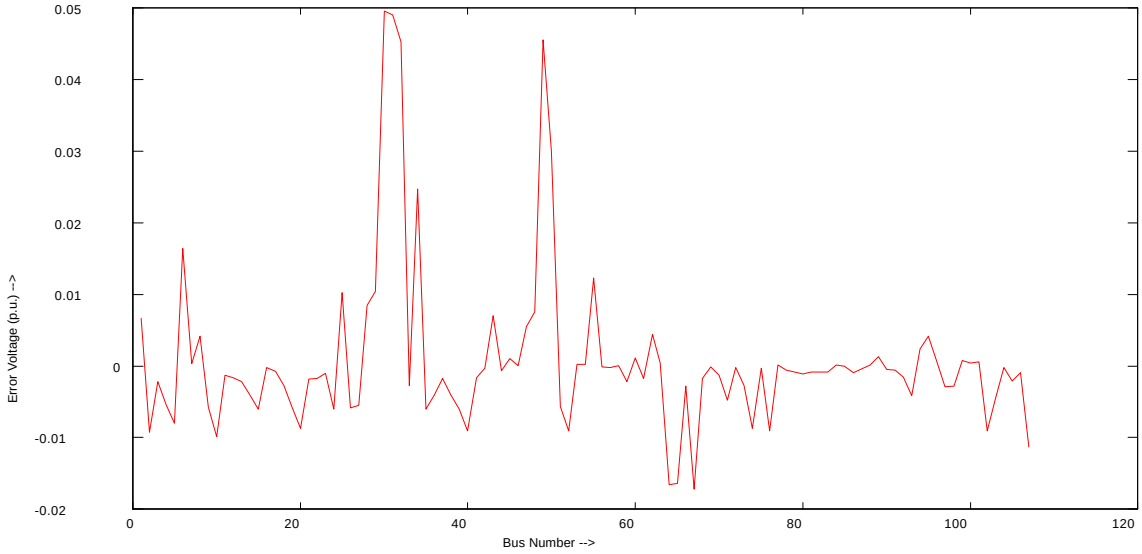

Figure 3.27 Line Outage Case 4 - Voltages

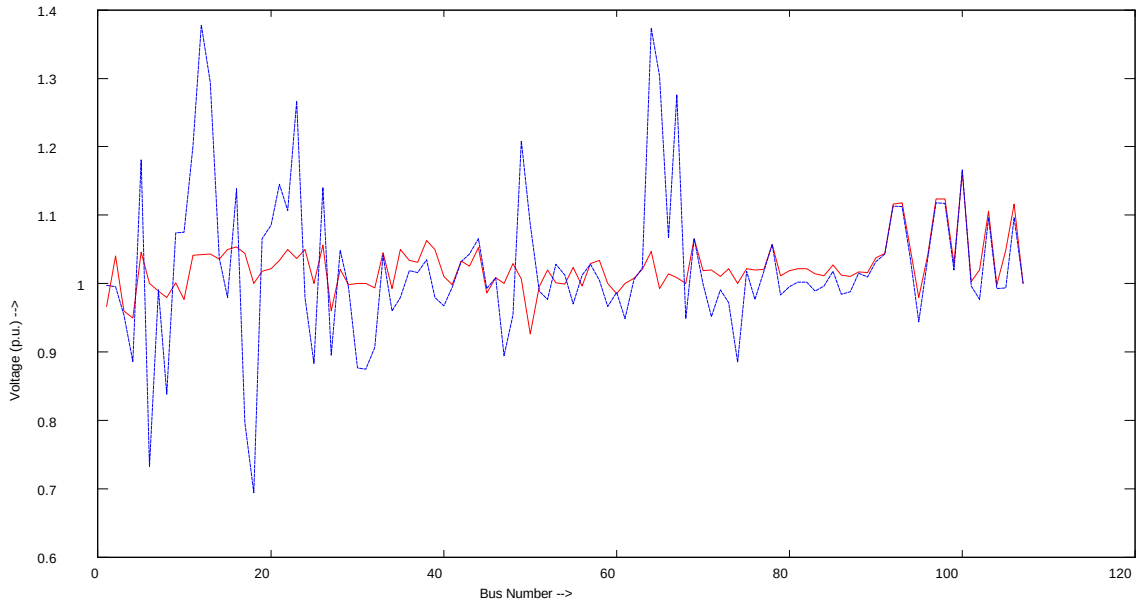

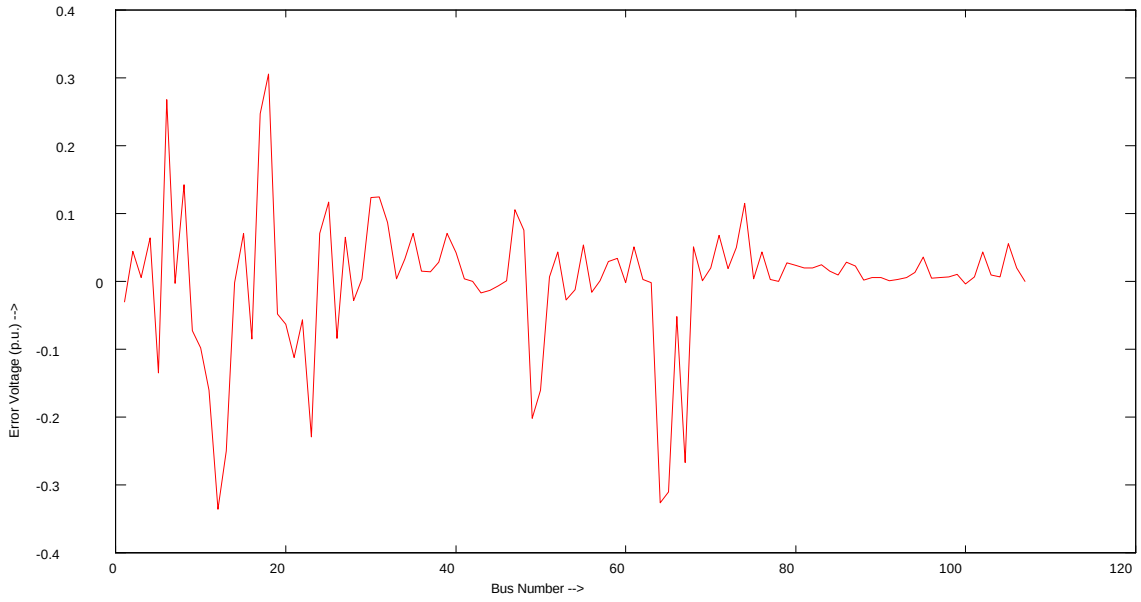

Figure 3.28 Line Outage Case 5 - Voltages

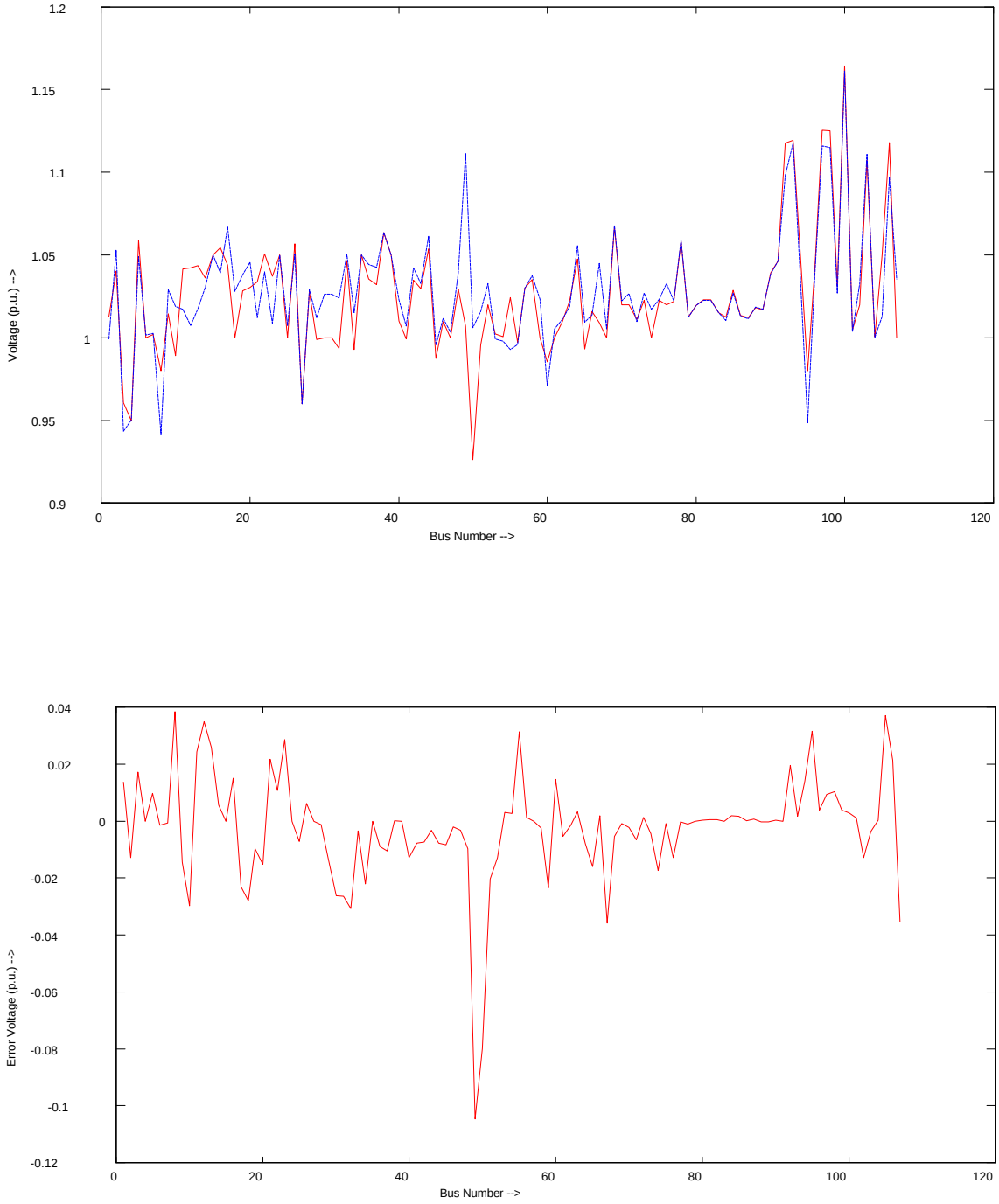

Figure 3.29 Line Outage Case 6 - Voltages

3.7 Series Compensator Buses:

The system has 52 buses where a series capacitor is connected to a transmission line. These buses do not have any loads or other branches connected to them. The voltages and angles at these buses can be calculated once the other unknown bus voltages have been calculated. Figure 4.2 shows the basic connection of all such buses. These buses could have been included for calculation by the coefficient matrix. However, the following approach is more accurate.

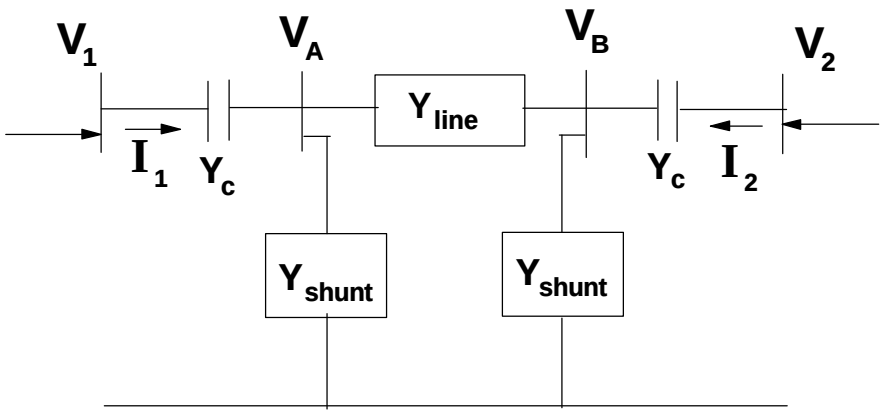

Figure 3.30 Series Capacitor Buses

A mathematical relationship can describe V_A and V_B in terms of V_1 and V_2. Thus it is only necessary to estimate V_1 and V_2 from the measured phasors and the voltages V_A and V_B can be determined as follows. The admittance matrix of the network is

$$\begin{vmatrix} Y_c & 0 & -Y_c & 0 \\ 0 & Y_c & 0 & -Y_c \\ -Y_c & 0 & Y_l+Y_c+Y_s & -Y_l \\ 0 & -Y_c & -Y_l & Y_l+Y_c+Y_s \end{vmatrix}$$

$$\begin{bmatrix} I_1 \\ I_2 \\ 0 \\ 0 \end{bmatrix} \quad \left[\begin{array}{cc} Y_{xx} & Y_{xy} \\ \hline Y_{yx} & Y_{yy} \end{array}\right] \quad \begin{bmatrix} V_1 \\ V_2 \\ V_A \\ V_B \end{bmatrix}$$

Solving the last two equations gives us the following relationships:

$$V_A = \frac{V_1(Y_c Y_l) + V_2 Y_c(Y_c + Y_l + Y_s)}{(Y_c + 2Y_l + Y_s)(Y_c + Y_s)} \tag{3.6}$$

$$V_B = \frac{V_2(Y_c Y_l) + V_1 Y_c(Y_c + Y_l + Y_s)}{(Y_c + 2Y_l + Y_s)(Y_c + Y_s)} \tag{3.7}$$

Using these two equations will yield the positive sequence voltage phasors at the intermediate capacitor buses.

3.8 Winter Time Load Flow Case

A load flow case based on load situation in the month of december was used to test the suitability of this A matrix. However, the loading pattern seems to be significantly different

from the summer time base load case used to develop the A matrix. The results of that case are as shown in the fllowing figures. The red or the dashed line is the estimated angles, the blue or solid line is the actual angles in the following plots.

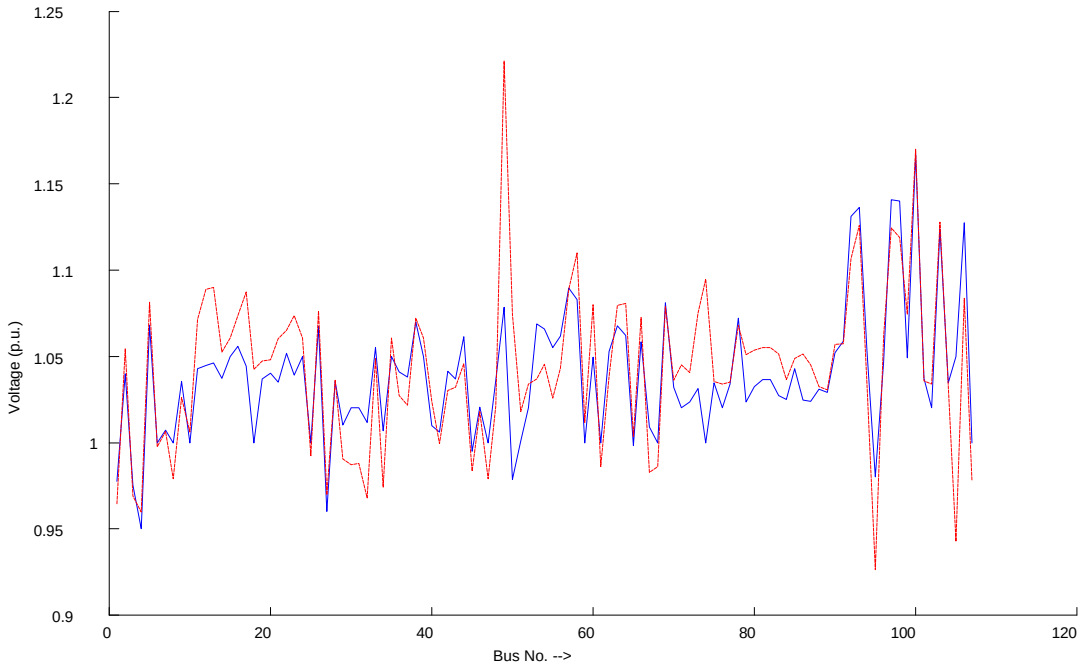

Figure 3.31 Winter Case Estimated and Actual Voltages

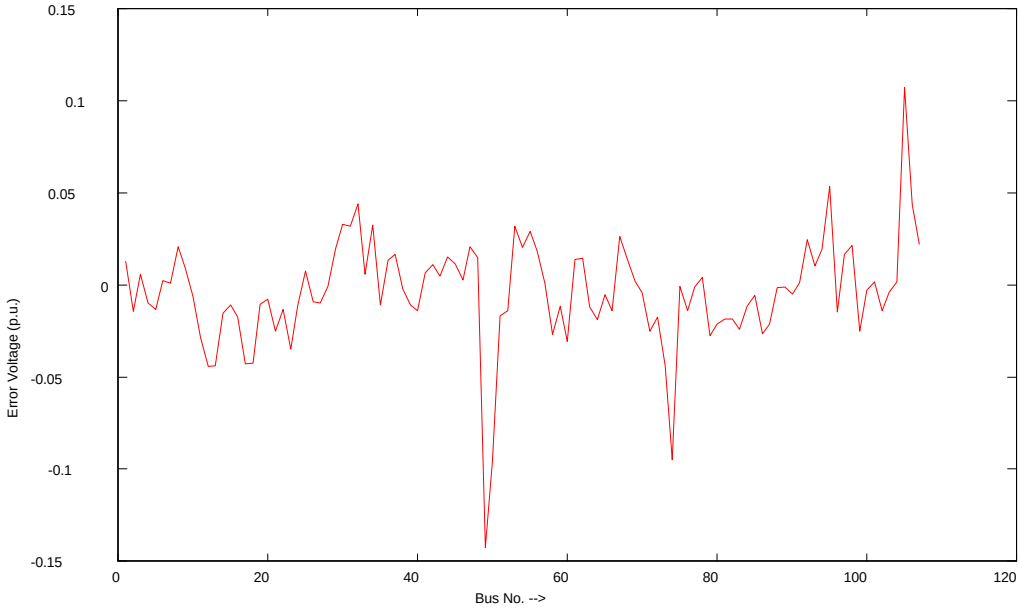

Figure 3.32 Error in Estimation of Winter Case Voltages

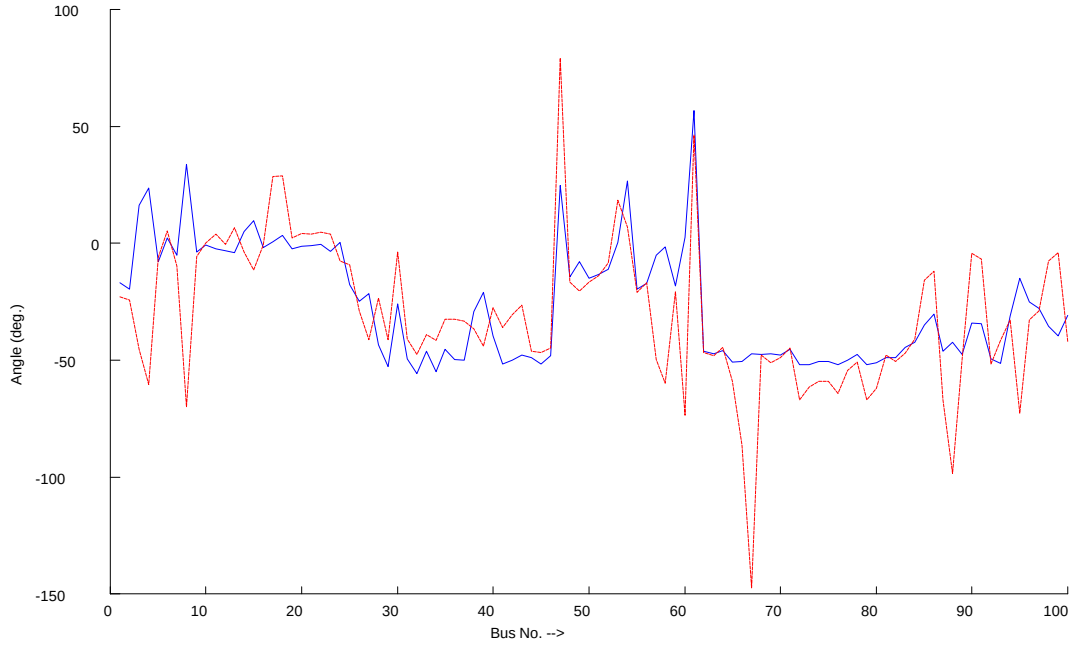

Figure 3.33 Winter Case Estimated and Actual Angles

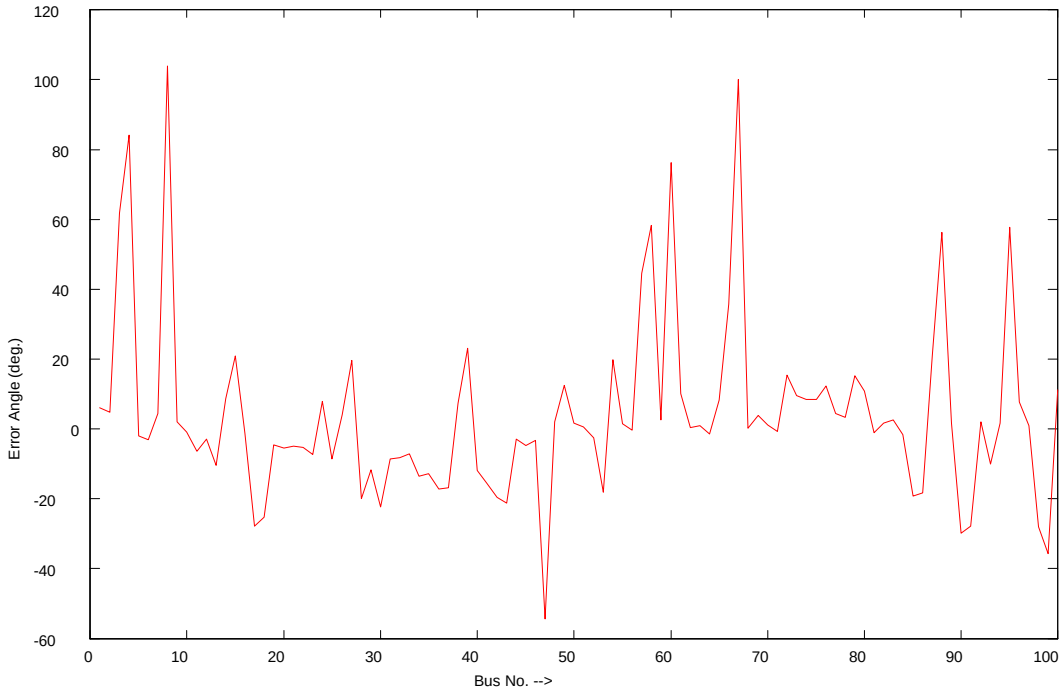

Figure 3.34 Error in Estimation of Winter Case Angles

The figures for angles do not show six buses in the Canada region because the error at these buses is very large and it makes comparison of estimated and actual angles at other buses difficult to read. It was observed that the estimated angles at certain buses had a large error. On closer observation of the A-matrix, these buses revealed a high dependence of these angles on one or two buses. Some of the coefficients in the rows of A-matrix were as high as 11. A new A matrix for angles was then created by including the winter time base case within the process of calculation of A-matrix. Thereafter, the angles were estimated using this A-matrix. The results are greatly improved as evident in the following figures.

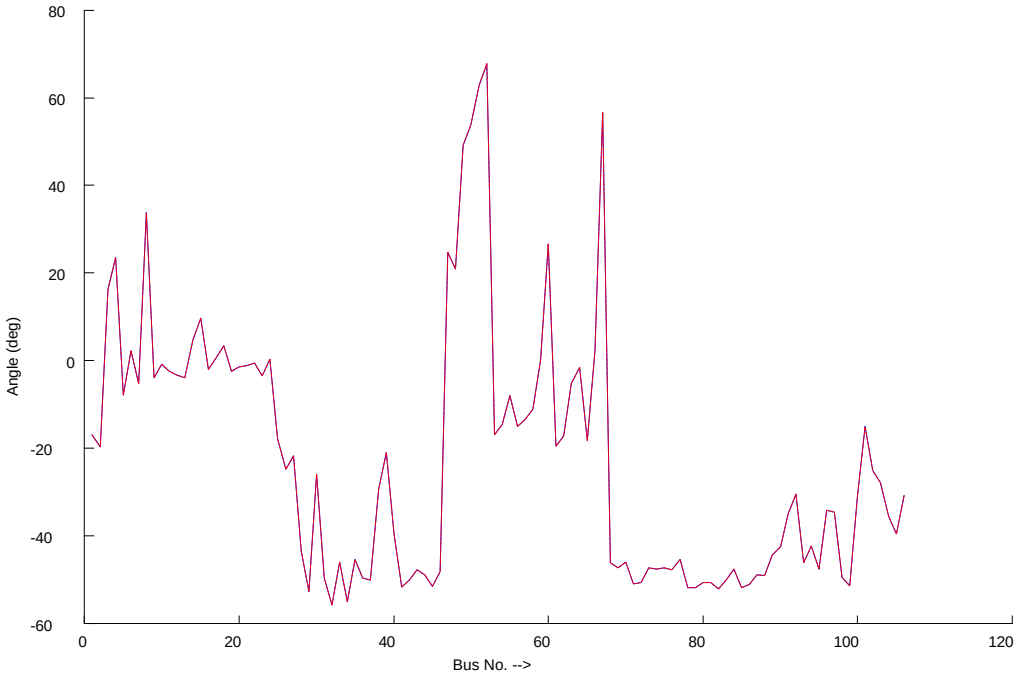

Figure 3.35 Winter Case Angles Estimated Using New A-Matrix

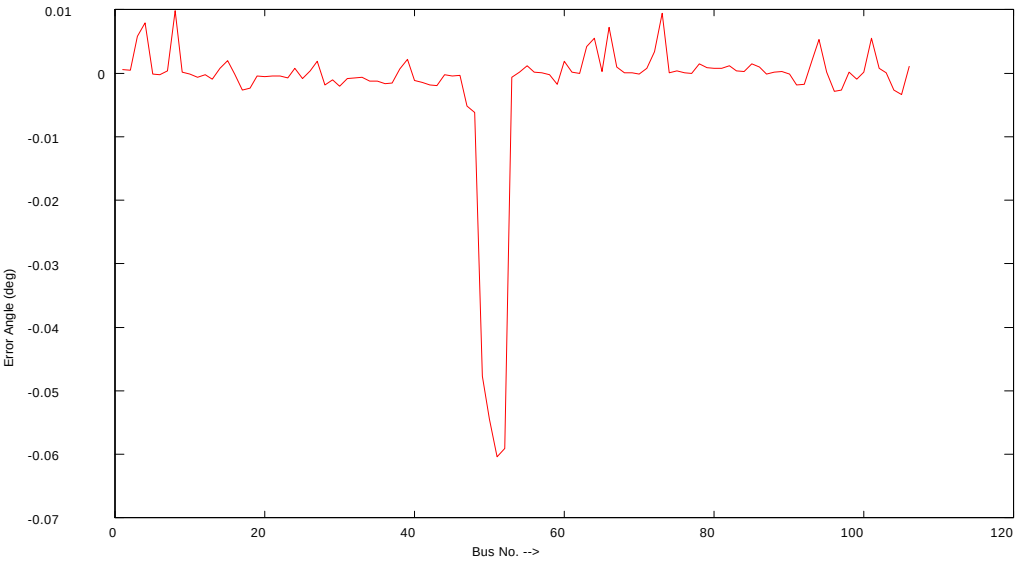

Figure 3.36 Error in Estimation of Angles with the New A-Matrix

The errors are greatly reduced. However, this may not necessarily indicate an improvement in the estimation capability of the A matrix. A case included in derivation of A-matrix when tested with the same A-matrix is likely to yield near perfect results. But it does serve to show that the more varied load flow cases one can include in the process of A-matrix calculation, enhanced is the capability of the matrix. To verify that the new matrix still works well with the summer time load flow cases, the first test case was tested again with the new A-matrix. The results of that run are as shown in the following figures.

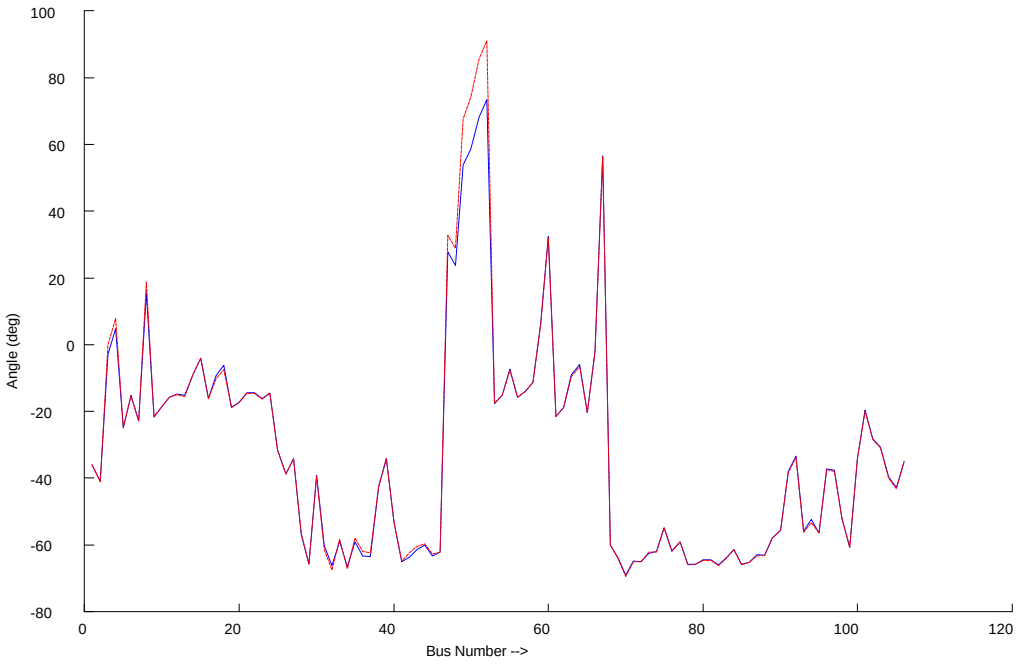

Figure 3.37 Test Case 1 Angles Estimated Using the New A-Matrix

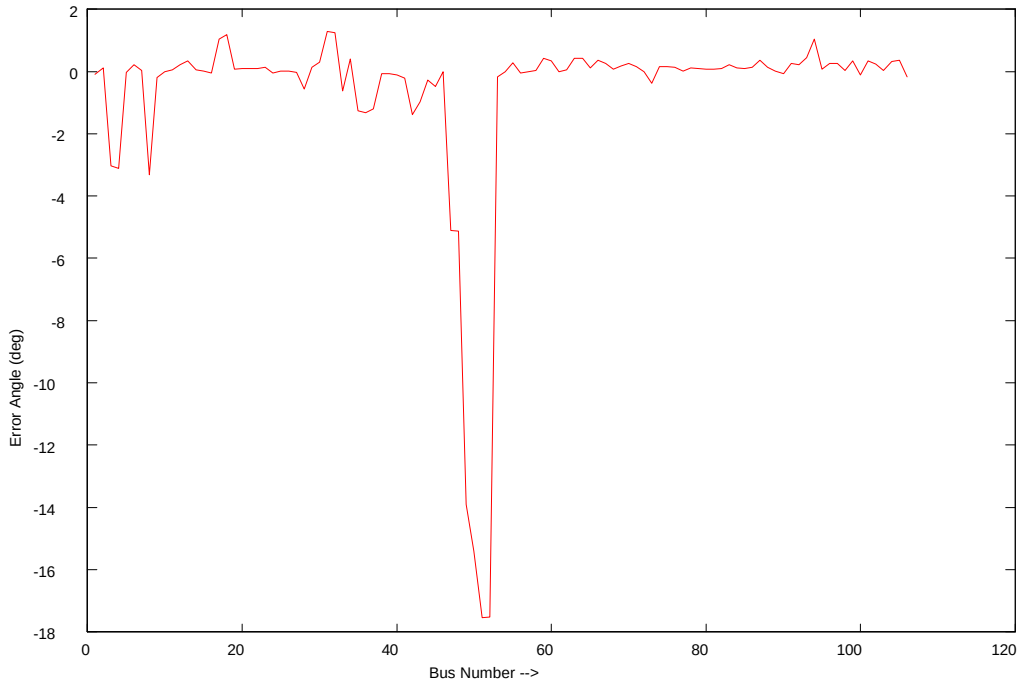

Figure 3.38 Error in Estimation of Test Case 1 Angles with the New A-Matrix

For comparison, the errors in angles in estimation of Test Case 1 angles with the original A-matrix are shown below in figure 3.8.6. A comparison shows that the errors in angle estimation of a summer test case are only slightly increased at some buses when the new A-matrix is used. Hence, we can safely conclude that the more different loading patterns are used in A-matrix calculation, the better the results can be in estimating phasors for a wide range of operating load conditions. However, a slight deprovement in angle estimation of summer time load cases because of inclusion of a winter case in A-matrix calculation can very well be an indication that it may be wise to formulate different A-matrices for different times of the year.

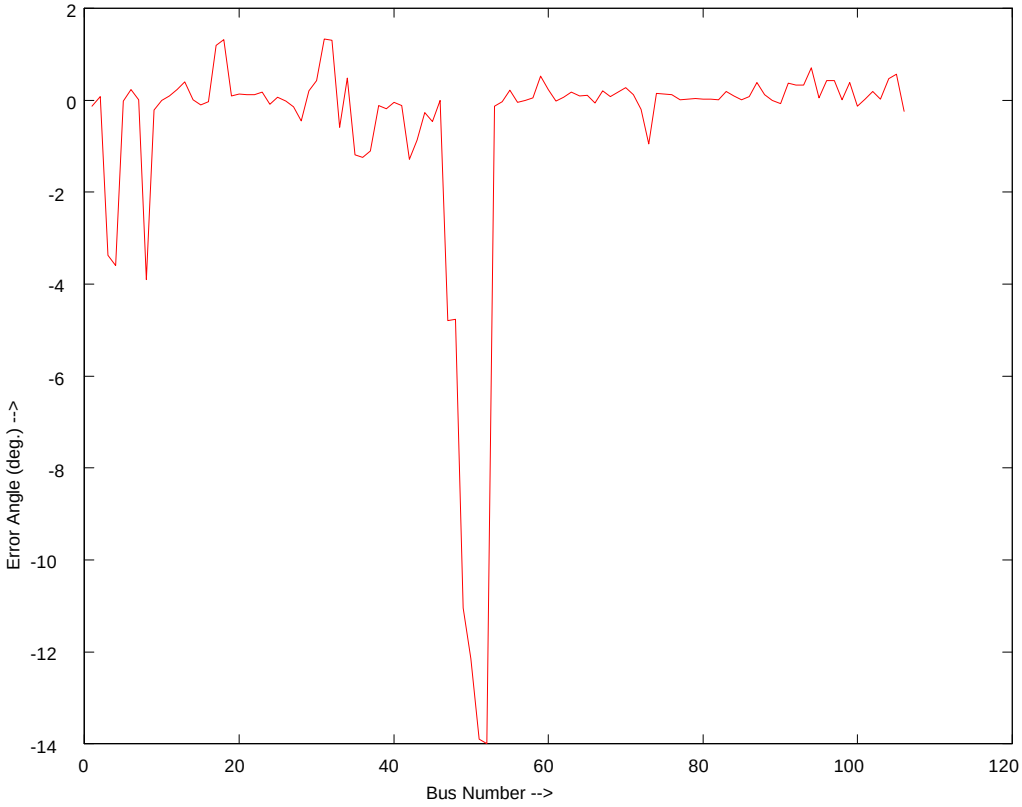

Figure 3.39 Error in Estimation of Test Case 1 Angles with the Old A-Matrix

4.
CONCLUSION AND FUTURE WORK

4.1 Conclusion

With the increasing use of computers and digital information in power systems, the availability of information about a system has become easier. Online data, artificial neural networks, fast computations and real time control are beginning to take over the theoretical and analytical solutions. However, the conventional methods of power system analysis still provide the element of theory to the latest methods of computations and estimations. Within this environment, there will be an increasing need of more and more such application oriented studies which can help minimize the resources and computation time. This study was intended to show that a small amount of real time information from limited resources can be expanded into a bigger picture of the whole system with simple relationships as derived herein. The study has been successful in its purpose, although more future work in this direction can improve the applicability of this research.

4.2 Future Work

Several experiments with this research as the starting point can be carried out to make further progress. A few ideas for the future are:

More theoretical investigation into the kind of relationship that phasors in neighbourhood are supposed to follow should improve results as well as the credibility of this approach. If the exact order of relationship can be determined theoretically, relationships of that order can be developed using appropriate number of different load flow cases instead of a simpler linear expression.

The amount of work involved in developing the load flow cases, solving them and organising the phasors will grow largely with increasing order of relationship being sought. However, this may not be required if phasor data can be directly collected from various sites at different times of a day on different days of a year. This will also provide a realistic picture of actual load variations and all possible variations. If more variations are required, some form of interpolation or extrapolation can yield more experimental cases. The stress should still be on covering all possible loading situations.

With data available, the overall system phasor picture can be recreated with the latest graphic algorithms. Also dividing the cases into seasonal or time of the day categories will become easier and derivation of different coefficient matrices for different times will become feasible.

With PMUs as the main resource and reason for this study, it would be a worthwhile effort to develop a method for optimal placement of PMUs with this purpose in mind. Although clustering will normally provide a similar placement, experiments to identfy prominent points in the network should help where clustering fails to give a distinct picture. It may also be worth putting some effort in investigating estimation errors at buses electrically far way from PMU buses. If a definite pattern indicating higher errors with increasing electrical distance is seen, the strategy of PMU placement can be designed around minimizing the overall system electrical distance from PMUs. In other words, the some of all impedances between each non PMU bus and its nearest PMU can be added up and a placement for which this total is minimum may be selected.

5.

REFERENCES

[1] IEEE Work Group, “Synchronized Sampling and Phasor Measurements for relaying and Control”, IEEE Transactions on Power Delivery Vol. 9, No. 1, January 1994, pg. 442-449.

[2] L.Mili, T.Baldwin and R.Adapa, “Phasor Measurement Placement for Voltage Stability Analysis of Power Systems”, 29th IEEE Conference on Decision and Control, Honolulu.

[3] T.Baldwin, “A Dual Search Method of Optimal PMU Placement for Complete Observability”, PhD Dissertation 1989, Dept. of Electrical Engineering, Virginia Polytechnique Institute and State University, Blacksburg.

VITA

Sunil Kabra was born in Udaipur, India on June 29, 1971. He did his Bachelor's in Electrical Engineering from the University of Roorkee, India. He attained the degree of Bachelor of Engineering in 1993. He joined Virginia Polytechnique Institute and State University in August 1993 as a full time student of Electrical Engineering working for a Master of Science degree. During his stay at Virginia Tech., he also served as a research assistant in the Power Systems Research Laboratory at Virginia Tech. His field of interest and area of research are Power System Protection, Relaying, Operation, Control and Stability.

Sunil is a member of the Institute of Electrical and Electronics Engineers.